Response to Referee #1

We thank Referee #1 for his comments and suggestions that, we believe, have helped improving the manuscript. We have addressed the comments point by point below. In addition, the errorbars shown on Fig. 9.b were modified, as those did not correspond to the actual variability of N_{50} absolute increase in the original version of the manuscript (former Fig. 8.b).

Comment 1: Classification of plume- vs non-plume days:
As the classification is critical for the statistical study, more details and illustrations are missing to describe and validate the classification of plume- vs non-plume days. As SO_2 represents indeed a clear tracer of the volcanic plume, a time series of SO2 mixing ratio values at Maido with highlighted volcanic events would be welcome in order to evaluate the amplitude of background variations in SO2 mixing ratios.
As this is the root of the paper, an illustration with AIS and DMPS observations for one representative strong plume day and one weakly influenced plume day before statistical representation of Fig. 1 would be required.

Reply 1: Adding a figure to support the method we followed to detect the volcanic eruption plume at the station, and to illustrate as well NPF events occurring in such unusual conditions, is in fact a good suggestion. Hence, we have included a new figure (Fig. 1) in the revised version of the manuscript, which displays a. The timeseries of the SO2 mixing ratio with some indication of the eruptive periods, b. AIS and DMPS observations showing an NPF event on a regular plume day and c. on a strong plume day.

Comment 2: Selection of plume-days, page 7, lines 19-27 : If I understand correctly, selected days are considered as 'plume-days' when at least one of the hourly averages of the SO2 mixing ratio exceeds 1 ppb over the 5 hours of interest each day (between 6 :00 and 11 :00 LT). The volcanic plume was detected during the 5 hours of the time window of interest for only 20 of the 36 'plume-days'. I am wondering if the authors should not restrict their study to these 'fully volcanically influenced days' ? If not, they should assess the impact of mixing in their study 'plume days' hours without any volcanic plume. This choice may artificially tend to decrease the difference between plume- and non plume-days.

Reply 2: We agree with the fact that including days with very short plume occurrence in the statistics did not give the most accurate picture of the volcanic eruption plume signature on NPF and related variables of interest. Hence, we have revised our classification to include only the days when the volcanic plume was detected over at least 3 hours between 06:00 and 11:00 LT. These days represent 80% of the former plume days (29/36); remaining 7 days with short plume occurrence, which are now excluded from the revised classification, were found in September and October. Corresponding statistics and results have been updated throughout the manuscript, but it is worth noticing that the main conclusions of this work were not affected.
Note that plume days were not restricted to the days when the plume was observed over the five hours of interest to allow a fair compromise between the number of plume days, that we wanted to keep sufficient for the relevance of our analysis, and significant influence of the volcanic eruption plume. Effect of the more "intense" plume conditions, both in terms of SO_2 levels and time duration of the plume occurrence, is further investigated by the mean of the so-called strong plume days.

Comment 3: Start time of NPF events, page 9:
Why are the detection and evaluation of the start time made by a visual inspection?
What is the difficulty in automating the detection of a concentration increase in the 1.5-2.5 nm range? Visual inspection is subject to large uncertainty and raise questions on the accuracy and reproducibility of the obtained results. An illustrative example would be also welcome to see how strong are the AIS/DMPS signals for days only poorly-contaminated by volcanic plumes.

Reply 3: The detection of the concentration increase could undoubtedly be automated, and recent studies have by the way reported different methods to allow for an automatic monitoring and description of NPF (eg: Hussein et al., 2005; Dall'Osto et al., 2017; Dada et al., 2018). Nonetheless, to our knowledge, the visual approach for the identification and analysis of NPF has, to date, been the most commonly used and is still popular. This is for instance illustrated by the very recent study by Hakala et al. (2019), who visually determined 4 different times to describe the progression of each NPF event. There is for

1

sure an uncertainty which is associated to this analysis "by eye", but we believe that such approach is less risky than automated ones with respect to more "critical" errors. In our case, such error could for instance be the detection of a concentration increase which is not connected to any clear NPF event.

As previously mentioned in Reply 1, an additional figure was added (Fig. 1) in the revised version of the manuscript to illustrate the NPF process in plume conditions.

Comment 4: Particle growth rate, pages 10-11:

Comment 4.A: Page 10, lines 3-8: The authors do not highlight any impact of the volcanic plume on the particle growth rate between 12 and 19 nm. The interpretation of the authors is that it may be difficult to clearly identify the impact of volcanic plumes at the Maido Observatory as the atmospheric dynamics is complex around this site and there may be an importation of growing particles likely transported to this site. The same processes (of imported particles, including potentially biomass burning aerosols as mentioned for CS variations in Sept and Oct) could also bias the observations of J2 and J12? The authors should comment on this and propose some solutions to 'clean' data by removing periods with strong influences by other sources of aerosols (urban, biomass burning, etc..).

Reply 4.A: It is absolutely true that, while affecting the determination of the particle growth, complex topography and atmospheric dynamics in turn also affect the calculation of particle formation rates. This is now clearly stated in Section 3.1.3: *"However, assessing the real effect of these specific conditions on the particle formation and growth is challenging"*. Also, following a comment from Referee #2, we have included an additional discussion in Section 3.1.3 to explain the limited effect of the plume on measured growth rates: *"This observation is most likely related to the fact that not only the amount of precursor vapours (including for instance SO2, see Fig. 1.a) was increased in the volcanic plume, but also the number concentration of the particles to grow, from both primary and secondary origin, as also reflected in the variations of the CS (Section 3.2.1) and discussed later in Section 3.3.1"*.
Instead of cleaning the data and removing some periods, the best would be to be able to evaluate the contribution of the different sources to the observed NPF events, and in turn to GR and J, in the same manner we have discussed the particle size distributions in Section 3.3.1. This is however much more complex for J and GR, and such detailed analysis of the impact of different conditions (anthropogenic air masses, biomass burning…) is anyway beyond the scope of the present study. Instead, our main goal was only to evaluate the effect of the plume conditions on J and GR in comparison with non-plume days. For that purpose, we have used a statistical approach, which allows for the comparison of a number of plume and non-plume days which is assumed to be sufficient to smooth the specificities of each single event with respect to all conditions other than plume occurrence.

Comment 4.B: Clearly higher values of J2 and J12 values are not observed under volcanic influence for the month of Sept. A clear volcanic signature is not identified either for J2 values for the month of Oct (with also surprisingly very spread J2 values for strong plume days). The authors should describe these discrepancies in the text and provide some interpretations or suggestions of interpretation (impact of biomass burning activities, or others?).
By contrast, page 10, lines 9-14: why is observed in May so much increase in J2 and J12 values for plume-days compared to non-plume days? Is there a specificity of the volcanic events, or of the meteorological conditions occuring in May? Opposite case: why is not observed an obvious distinct behaviour of plume-days in Oct?

Reply 4.B: It is true that we should have commented more on the comparison between the formation rates measured in and off- plume conditions, as different trends are effectively highlighted in this study. We have thus included a paragraph in Section 3.2.1, which discusses the variability of CS, together with that of SO$_2$ mixing ratio, as we believe they are key parameters driving the variations of J$_{12}$ and J$_2$. This discussion also refers to the variations of the particle growth rate, in response to one of the comments from Referee #2: *"In addition, the balance between the amount of SO$_2$ and the magnitude of the CS most likely influenced the strength of the observed events, and explained in specific the variable trends highlighted earlier in the comparison of the particle formation rates calculated on plume and non-plume days (see Sect. 3.1.3, Fig. 3.b and c). Indeed, as reported previously, the largest CS increase observed between non-plume and plume NPF event days occurred in May, when SO$_2$ mixing ratios were also the highest (Fig. 1), with a median of 26.7 ppb [25th percentile: 1.1 ppb; 75th percentile:*

120.5 ppb] calculated during nucleation hours (06:00 and 11:00 LT). We may thus hypothesize that the resulting conditions were highly favourable to NPF, and not only lead to high NPF frequency (Fig. 2), but also to stronger events, with increased particle formation rates compared to non-plume days (Fig. 3.b and c). In September and October, the median CS measured in plume conditions were comparable to that observed in May (Fig. 4.a), but SO_2 mixing ratios were in contrast lower during
5 *nucleation hours, with medians around 3.4 ppb [1.5 ppb; 5.6 ppb] and 3.8 ppb [1.9 ppb; 16.9 ppb], respectively. This most likely resulted in less favourable conditions for NPF than in May, which in turn did not enhance the particle formation rates compared to non-plume days. Higher CS observed on plume days also supported the fact that in plume conditions, as suggested in the previous section, the number of particles to grow was increased compared to non-plume days, and the concurrent strengthening of the precursor source rate was on average not sufficient to result in faster particle growth. Nonetheless, while*
10 *it was possible to evidence the abovementioned trends with our statistical approach, one should keep in mind that both the occurrence and characteristics of NPF are likely to be affected at very short time scales due to the variable nature of the volcanic eruption. Deeper investigation of the effect of the volcanic eruption plume on NPF would thus require more detailed analysis of the event to event variability, which was however beyond the scope of the present work".*

15 **Comment 4.C**: More generally, the authors should discuss the advantages and also the disadvantages or limitations to have data collected at a high altitude atmospheric observatory and the potential biases that may affect the results at such a site (including complex atmospheric dynamics, fluctuating relative humidity, is it easier or not to identify imported species, a less polluted background or not, etc…).

20 **Reply 4.C**: We believe that the main specificities of a site such as the Maïdo which were relevant to the present work have been mentioned in the manuscript, including in particular the complex topography and atmospheric dynamics which affect the transport of both NPF gaseous precursors an growing/pre-existing particles, with consequent effect on NPF characteristics, particle size distribution and in turn CCN population. Deeper analysis of the advantages/disadvantages of high altitude observatories is behind the scope of the present work; it is however of high interest, and is the main focus of a review dedicated
25 to the observation of NPF from such high altitude sites, currently in preparation.

Comment 5: Which is the impact of relative humidity on NPF? As relative humidity is measured at Maido, is there any correlation with NPF? Are observed higher RH values during plume-days (as the Piton de la Fournaise plume may be rich in volcanic water vapour) or not?
30
Reply 5: The effect of RH on NPF is not plain to understand, as contrasting observations have been reported, regarding in specific its influence on the particle formation rates (e.g. Birmili et al., 2003; Duplissy et al., 2016). We have investigated the variations of RH observed at Maïdo on event days, in and off-plume conditions, and on non-event days, together with that of temperature and radiation, which are also reported as key meteorological parameters. The results of this analysis are reported
35 at the beginning of Section 3.2: *"NPF has been previously reported to be influenced by various atmospheric parameters, including solar radiation, temperature (Dada et al., 2017), as well as RH, which effect on the process is certainly the less evident to predict and understand (e.g. Birmili et al., 2003; Duplissy et al., 2016). In the frame of the present analysis, the median diurnal variations of the abovementioned parameters reported on Fig. S1 (in the Supplementary) did not highlight any specificity for the events observed on plume days, and displayed similar behaviour in and off-plume conditions".*
40 A corresponding figure showing the median diurnal patterns of temperature, RH and global radiation measured in the different conditions (non-event days, event days in and off-plume) was included in the Supplementary; note that all the figures originally shown in the different Appendices were moved to the Supplementary in order not to multiply the number of Appendices.

Comment 6: Impact of condensation sink (CS) page 11:
45 Right of Fig. 3: in the plot of CS vs SO2 mixing ratio for plume-days and strong-plume days, could it be added non-plume days to assess if obvious differences are observed between plume- and non plume-days in this representation?
Left of Fig. 3: how do the authors explain the large CS observed in Sept and Oct for
non-plume days?

Reply 6: It was unfortunately not possible to include non-plume days in Fig. 4.b (former Fig. 3.b) because SO_2 mixing ratios were mostly below the detection limit of the instrument outside of the eruptive periods, as indicated in Section 2.1: *"The detection limit of the instrument was about 0.5 ppb, which is above the usual SO2 mixing ratios encountered at Maïdo outside of the eruptive periods of the Piton de la Fournaise (see Fig. A1 in Foucart et al. 2018)"*. This is now also recalled in Section 2.3: *"The relatively low SO_2 mixing ratios observed outside of the eruptive periods, <u>mostly below the detection limit of the instrument</u>, reflect the low pollution levels characteristic of this insular station, located at high altitude in a region rarely subject to significant influence of pollution from continental origin"*.

Detailed investigation of the origin of the large CS observed on non-event days in September and October was behind the scope of the present work, nonetheless this observation is already briefly discussed in the manuscript (Section 3.2.1) : *"Indeed, comparable median CS were observed in August regardless the occurrence of NPF later during the day, higher values were in contrast obtained on event days in May, <u>while the opposite was observed in September and October, most likely related to biomass burning activity in South Africa and Madagascar during austral spring</u> (Clain et al., 2009; Duflot et al., 2010; Vigouroux et al., 2012)."*

Comment 7: Relationship between J2 and [H2SO4], page 12:

According to Fig. 4, a correlation relationship between J2 and [H2SO4] is not obvious: data points are very scattered, as illustrated by the very low value of R2 of 0.21 and 0.11 for all plume and strong-plume days respectively. In this context, is it meaningful to try to fit anyway a correlation relationship and estimate k and a coefficient?

Moreover, except higher concentrations of H2SO4, data associated to strong-plume days do not seem to present a very different relationship between J2 and [H2SO4] (Fig. 4a). The weak difference in the relationship which is retrieved seems just to result from the influence of 3 points, potentially outliers? If these points would have been represented in black, and not in yellow, it would be very difficult to distinguish any different behaviour.

Reply 7: The correlation between J_2 and $[H_2SO_4]$ derived from data measured on all plume days is definitely moderate but still significant, as indicated by the corresponding p-value (2.35×10^{-24}). Regarding strong plume days, we found a mistake in the selection of the data points for the fitting procedure. Using the correct data finally lead to very similar fit parameters to that obtained for all plume days, which is now explicitly mentioned in the revised version of the manuscript: *"the relationship between J_2 and [H2SO4] did not appear to be significantly different on strong plume days compared to regular plume conditions"*. For that reason (and also for more clarity) strong plume days are not any longer highlighted on Fig. 5. Additional discussion regarding the contributions of charged and neutral nucleation pathways was also included in Section 3.2.2, based on the use of the parameterisation by Määtänen et al. (2018): *"As evidenced on Fig. 5.a, the total formation rate of 2 nm-clusters was mostly explained by ion induced nucleation for [H2SO4] below ~ 8×108 cm-3, while neutral pathways seemed to explain the observations at larger sulfuric acid concentrations"*.

Also, since the results reported in Sections 3.1 and 3.2 only revealed limited signature of strong plume conditions on NPF characteristics (and related parameters of interest), we have decided not to put any focus on these specific days in the last Section (3.3) in order to make our message as clear as possible.

Minor comments:

Comment 1: 'Active volcanic plume': I do not understand this term. Given lines 31-32 in the introduction, I am wondering if the authors may want to refer to a volcanic plume emitted during an eruption compared to passive degassing emitted out of eruptive periods. If so, please refer rather to 'volcanic eruption plume'

Reply 1: Changed throughout the manuscript.

Comment 2: Page3,lines5-8: 'primary particles are fragment of ash while secondary particles...' : Volcanic primary particles do not include only ash particles but also sulfate aerosols, as illustrated by near-source measurements (e.g. refer to first publications on this matter which include Allen et al., 2002 ; Mather et al., 2003, 2004, etc..).

Reply 2: We thank the reviewer for pointing out this omission. This has been addressed in the revised version of the manuscript:

- In the introduction: *"Primary sulphate aerosols of volcanic origin were also evidenced by near source measurements conducted at Masaya volcano by Allen et al. (2002), who were however not able to identify their precise mechanisms of formation. Several pathways were later suggested for the formation of H2SO4 at the vent, including catalytic oxidation of SO2 inside the volcanic dome Zelenski et al. (2015), high temperature chemistry in the gas phase (Roberts et al., 2019), as well as aqueous production of H2SO4 from SO2 (Tulet et al., 2017). H2SO4 produced by the mean of the aforementioned reactions is expected to contribute to the formation and growth of particles in the close vicinity of the volcano, which are in turn assimilated to primary volcanic aerosols"*.

- In Section 3.2.1: *"This nomenclature is consistent with earlier results from Allen et al. (2002), who reported the presence of primary sulphate aerosols at Masaya volcano"*.

Comment 3: 'Here we report observations of NPF performed at the high-altitude observatory of Maïdo (2165 m a.s.l., La Réunion Island) between 1st January and 31st December 2015. During this period of time, 3 effusive eruptions of the Piton de la Fournaise, located 39 km away from the station, were observed and documented, resulting in 36 days of measurement in volcanic plume conditions to be compared with 250 "non -plume days'. 250 + 26 = 276 days, what happens with the missing 89 (=365-276) days?

Reply 3: It is true that the reported numbers were somewhat confusing and needed some clarification, now available in Section 2.3: *"In the end, after filtering the data for instrument malfunctioning and / or absence of measurements (71 days in total), 29 plume days and 250 non-plume days were included in the analysis. The 15 remaining days, with late or short plume occurrence, will not be further discussed"*.

Comment 4: There are many references to a study in preparation (Sahyoun et al., in prep) which is presented as an earlier work: has this paper been submitted to a journal with open discussion where it would be accessible or has it been published since then? If yes, please update so that the reader can have access to this manuscript.

Reply 4: This paper was indeed not published when we first submitted our manuscript. We have now included the reference: Sahyoun, M., Freney, E., Brito, J., Duplissy, J., Gouhier, M., Colomb, A., Dupuy, R., Bourianne, T., Nowak, J. B., Yan, C., Petäjä, T., Kulmala, M., Schwarzenboeck, A., Planche, C. and Sellegri, K. : Evidence of new particle formation within Etna and Stromboli volcanic plumes and its parameterization from airborne in-situ measurements, J. Geophys. Res.-Atmos, https://doi.org/10.1029/2018JD028882, 2019.

Comment 5: Abstract is very long, if possible you should try to shorten it (possibly remove the mention to the correlation relationship between J_2 and H_2SO_4 concentration which does not seem obvious (as developed above).

Reply 5: The abstract is indeed quite long, but we believe it gives the opportunity to the readers (who are nowadays often busy!!) to quickly get the storyline and main results of this work.

Comment 6: Please reformulate these sentences for clarity:
1) abstract, Page 1, line 17 : 'as those form the baseline to calculate..'
2) abstract, Page 1, line 30 : 'recorded in the different conditions': recorded in the different conditions described thereafter..
3) abstract, Page 1, line 26-27: 'compared to non-plume days, during which condensable species were in contrast transported from lower altitude by the mean of convective processes': it is difficult to understand the meaning of this sentence if we have not read the manuscript yet.
4) Page 2, lines 21-22 : 'the radiative forcing... still has a large uncertainty'
5) Page 11, line 16 : 'loss rate of the vapours' ? What do you mean by 'vapours'?

Reply 6:

1) This part of the sentence was removed as the information it contains is not of the highest importance for the abstract. This topic is further discussed in the introduction.
2) Changed to: "based on the analysis and fitting of the particle size distributions recorded in and off-plume conditions".
3) For more clarity this part of the sentence was also removed from the abstract; corresponding results are discussed in details in the manuscript.
4) Changed to "the radiative forcing associated to these effects (usually referred to as "indirect effect") is known with a still large uncertainty".
5) Changed to "the strengthened loss rate of the condensing vapours involved in particle formation and growth".

References:

Birmili, W., Berresheim, H., Plass-Dülmer, C., Elste, T., Gilge, S., Wiedensohler, A., and Uhrner, U.: The Hohenpeissenberg aerosol formation experiment (HAFEX): a long-term study including size-resolved aerosol, H2SO4, OH, and monoterpenes measurements, Atmos. Chem. Phys., 3, 361-376, https://doi.org/10.5194/acp-3-361-2003, 2003.

Dada, L., Chellapermal, R., Buenrostro Mazon, S., Paasonen, P., Lampilahti, J., Manninen, H. E., Junninen, H., Petäjä, T., Kerminen, V.-M., and Kulmala, M.: Refined classification and characterization of atmospheric new-particle formation events using air ions, Atmos. Chem. Phys., 18, 17883-17893, https://doi.org/10.5194/acp-18-17883-2018, 2018.

Dall'Osto, M., Beddows, D. C. S., Asmi, A., Poulain, L., Hao, L., Freney, E., Allan, J. D., Canagaratna, M., Crippa, M., Bianchi, F., de Leeuw, G., Eriksson, A., Swietlicki, E., Hansson, H. C., Henzing, J. S., Granier, C., Zemankova, K., Laj, P., Onasch, T., Prevot, A., Putaud, J. P., Sellegri, K., Vidal, M., Virtanen, A., Simo, R., Worsnop, D., O'Dowd, C., Kulmala, M. and Harrison, Roy M.: Novel insights on new particle formation derived from a pan-european observing system, Scientific Reports, 8, 1482, 2018.

Duplissy, J., Merikanto, J., Franchin, A., Tsagkogeorgas, G., Kangasluoma, J., Wimmer, D., Vuollekoski, H., Schobesberger, S., Lehtipalo, K., Flagan, R. C., Brus, D., Donahue, N. M., Vehkamäki, H., Almeida, J., Amorim, A., Barmet, P., Bianchi, F., Breitenlechner, M., Dunne, E. M., Guida, R., Henschel, H., Junninen, H., Kirkby, J., Kürten, A., Kupc, A., Määttänen, A., Makhmutov, V., Mathot, S., Nieminen, T., Onnela, A., Praplan, A. P., Riccobono, F., Rondo, L., Steiner, G., Tome, A., Walther, H., Baltensperger, U., Carslaw, K. S., Dommen, J., Hansel, A., Petäjä, T., Sipilä, M., Stratmann, F., Vrtala, A., Wagwww.atmos-chem-phys.net/17/14171/2017/ Atmos. Chem. Phys., 17, 14171–14180, 2017 14178 J. Lengyel et al.: Electron-induced chemistry in microhydrated sulfuric acid clusters ner, P. E., Worsnop, D. R., Curtius, J., and Kulmala, M.: Effect of ions on sulfuric acid-water binary particle formation: 2. Experimental data and comparison with QC-normalized classical nucleation theory, J. Geophys. Res.-Atmos., 121, 1752–1775, https://doi.org/10.1002/2015JD023539, 2016.

Hussein, T., Dal Maso, M., Petaja, T., Koponen, I. K., Paatero, P., Aalto, P. P., Hameri, K., and Kulmala, M.: Evaluation of an automatic algorithm for fitting the particle number size distributions, Boreal Environ Res, 10, 337-355, 2005.

Response to Referee #2

We thank Referee #2 for his comments and suggestions, which we hope will help improving the manuscript. We have addressed the comments point by point below, with separate answers to the different topics/aspects of each of the main comments (1-3). In addition, the errorbars shown on Fig. 9.b were modified, as those did not correspond to the actual variability of N_{50} absolute increase in the original version of the manuscript (former Fig. 8.b).

Comment 1: Section 2.2. The authors should discuss briefly the uncertainties and limitations of the equations 1 to 4 in calculating the particle formation (J) and growth (GR) rates in their data. **(A)** First, these equations have been developed originally for regional NPF, in which formation and growth of particles is assumed to take place relatively homogeneously over large spatial scales. This is apparently not the case in plumes where, among other things, various transport effects on J and GR should be taken into account. **(B)** Second, experimental limitations cause further uncertainties in determining J and GR. For example, using coagulation sink at 12 nm for all particles in the size range 12-19 nm in equation 1 causes some overestimation of coagulation losses, which results in underestimating J12. Also, Calculating J2 from J12 would require knowing GR in the size range 2-12 nm rather than that in the size range 12-19nm. While it is impossible to take into account the above issues to correct the data, the authors should at the very least discuss these issues briefly in section 2.2. If possible, the authors could also estimate whether resulting uncertainties are important or not with respect to their results.

Reply 1:

(A) This is an interesting discussion, as it is true that the abovementioned equations were originally derived to describe regional NPF. However, we do find a stronger increase of N_{12-19} over time within the volcanic plume compared to non-plume conditions. The resulting increased particle formation rates observed on plume days indicate that particles are formed within the volcanic eruption plume "homogeneously" along the transport pathway to Maïdo. The same reasoning can be done with the growth rate. If nucleated particle appear to gradually "grow" with the typical banana shape, it means that the regional-type nucleation and growth process is taking place along the transport path. Based on these observations, we believe that Eq. (1-4) can be used to describe such events occurring at a sub-regional scale. This aspect is now better addressed in Section 3.1.3: *"Higher particle formation rates observed on plume days indicate that particles were constantly formed in the volcanic plume along the transport pathway to Maïdo, showing that nucleation and growth taking place over a distance of the order of 40 km appears like a regional scale homogeneous process, which can be described with the usual equations (Eq. 1-4) recalled in Section 2.2".*

(B) In fact, the use of $CoagS_{12}$ for all particles in the investigated size range leads to some uncertainty in the calculation of J_{12}. However, based on Eq. (1), which is recalled below, we believe that $CoagS_{12}$ contributes to an overestimation (and not underestimation) of the particle formation rates.

$$J_{12} = \frac{dN_{12-19}}{dt} + CoagS_{12} \times N_{12-19} + \frac{GR_{12-19}}{7\ nm} \times N_{12-19} \qquad (1)$$

This is now clearly mentioned in Section 2.2: *« Note that the use of $CoagS_{12}$ for all particles in the range between 12 and 19 nm might cause some overestimation of the actual coagulation losses, and in turn lead to high estimates of J_{12}."* Also, we have included a sensitivity study at the end of Section 2.2 to give further insights into the effect of the particle growth rate in the determination of J_2 based on Eq. (2-4). All in all, this analysis reveals only limited effect of the growth rate variability/accuracy over the 2-19 nm in the conditions of our study.

Comment 2: Section 3.2.2. In this work, neither J2 nor H2SO4 concentration were measured directly, but were derived from other measured quantities, resulting in potentially large uncertainties in their values. This has implications which are not mentioned in the paper. **(A)** First, how reliable is the observed relation between J2 and H2SO4 concentration, and how

meaningful is it to compare this relation with those observed in studies were J and H2SO4 concentration were measured directly? **(B)** Second, how meaningful is it compare J obtained here with parameterized J due to binary water-sulfuric acid nucleation as a function of H2SO4 concentration? Does this comparison tell anything about nucleation mechanism?

5 **Reply 2**:

(A) We agree with the fact that the use of values derived from indirect calculations may lead to uncertainties, and such limitations should be kept in mind when interpreting the results. Regarding the determination of [H_2SO_4], we were unfortunately not able to evaluate the relevance of the proxy by Mikkonen et al. (2011) in volcanic plume conditions.
10 Hence, in addition to the comment reported in Section 3.2.2 (*"which may stem from a reduced predictive ability of the proxy by Mikkonen et al. (2011) for the highest SO₂ mixing ratios"*), we have included another "warning" earlier in the manuscript, in Section 2.4: *"However, since the relevance of this proxy could not be evaluated in volcanic eruption plume conditions, neither from available measurements nor existing literature, one should keep in mind the potential limits of using such parametrization when interpreting the related results".* Also, this demonstrates the need
15 for additional measurements, as now clearly indicated at the end of Section 3.2.2: *"Such measurements would also allow more detailed evaluation of the proxy by Mikkonen et al. (2011) for the prediction of [H₂SO₄] in volcanic eruption plume conditions".*

Concerning J_2, it goes without saying that the use of Eq. (2-4) naturally leads to some uncertainties in the calculation of J_2. However, these equations have already been approved and used in other studies, such as in the companion paper
20 by Foucart et al. (2018). Moreover, the impact of GR_{12-19} on the results derived from Eq. (2-4), which was rightly questionable, is now explicitly discussed in the revised version of the manuscript.

The results obtained in the present work were compared with that of other studies where measured values were used since those were the only "reference" we had for such comparison, in specific when restricting the literature to the poorly documented volcanic plume conditions. The comparison with Sahyoun et al. (2019) finally gave the chance to
25 highlight the similarity of the values derived from the different approaches (measured *vs* calculated J and [H_2SO_4]) in comparable conditions, thus giving more credit to the values reported in the present analysis.

(B) Comparison with the theory has multiple interests, as mentioned in the paper in Section 3.2.2:
- Investigate whether or not the binary water-sulfuric acid nucleation can explain the particle formation rates
30   reported in plume conditions;
- Show evidence for the ability of the parameterization to provide some reasonable estimates of the particle formation rates based on the knowledge of SO₂ mixing ratios only.

Based on the use of the parameterization, we have also included some additional discussions in the revised version of the manuscript regarding the contribution of the different nucleation mechanisms, charged and neutral (Section
35 3.2.2): *"As evidenced on Fig. 5.a, the total formation rate of 2 nm-clusters was mostly explained by ion induced nucleation for [H2SO4] below ~ 8×10⁸ cm-3, while neutral pathways seemed to explain the observations at larger sulfuric acid concentrations.".*

Finally, the fair agreement between the formation rates derived from measurements and that predicted by the theory gave additional support to our approach based on indirect measurements.

40

Comment 3: There are a few issues related to the particle growth that need some clarifications. **(A)** First, did the authors consider particle growth from one mode to another when estimating the relative contributions of primary and secondary particles in each mode? This remains a bit unclear when reading the results. **(B)** Second, the authors do not tell what were the typical air mass transport times from the volcano to the measurement site. This is important because for the reported particle
45 growth rates (Fig. 2a), it takes a while before particles formed in the plume are able to growth into the Aitken mode, and for several hours before they can reach the minimum CCN size (assumed >50 nm here) or the accumulation mode. Is it feasible that particle formed by NPF in the volcanic plume reach these sizes by the time measurements were conducted? **(C)** Third, while I agree with the authors that volcanic emissions are able to boost particle growth by e.g. heterogenous reactions of SO2 on particle surfaces, there seems to be some inconsistences in the storyline: on one hand the authors state that the plume appear

not to influence the particle growth (section3.1.3), and on the other hand they state that particle growth in the plume increased both modal (section 3.3.1) and CCN (section 3.3.2) concentrations.

(A) The evaluation of primary vs secondary processes contributing to volcanic emissions were performed via the comparison of the 7:00 LT size distribution in and out of plume to evaluate primary emissions, and via the comparison of the maximum particle concentrations measured for each mode in plume and out of plume (observed between 11:00 and 14:00 LT depending on the modes and conditions) for the secondary particle contribution. The presence of a secondary contribution to the accumulation modes is likely the result of the growth of particles from the Aitken mode, due to the presence of more condensable gases. This is now more clearly stated in the text, and also recalled in the caption of Fig. 8.

(B) We have included a discussion regarding the growth of the particles nucleated close to the vent during their transport to Maido in Section 3.1.3, showing evidence for their ability to reach ~50 nm, i.e. CCN relevant sizes, over the distance of 39 km between the volcano and the station: *"A rough estimate for the transport time of the particles nucleated in the vicinity of the volcano to the Maïdo observatory can be obtained by dividing the distance between the sites by the median wind speed measured on NPF event days: 39 km ÷ 1.8 m s-1 ≈ 6 hours. This indicates that in such conditions, the GR_(12-19) reported on Fig. 3.a were often sufficient (> 8 nm h-1) for the newly formed particles (~ 1 nm) to grow up to CCN relevant sizes (~ 50 nm, see Sect. 3.3.2) during their transport, further explaining the observation of the typical banana shape of the events, both on plume and non-plume days. Similar analysis was repeated with the 75th percentile of the wind speed measured on NPF event days (2.9 m s-1), and, again, the observed growth was often fast enough (> 13 nm h-1) for the particles to reach 50 nm during the corresponding ~ 3 hours 45 minutes trip to Maïdo".*

However, when focussing more specifically on the CCN population in Section 3.3.2, we did not try to isolate the contribution of NPF to the observed CCN increase, as this would have been complex (impossible?), but we reported instead the contribution of secondary particles. Indeed, we did select the days when particles originating from NPF reached CCN-size, and in turn presumably contribute to CCN population, but the concentration increase that we calculated reflected the contribution of secondary processes as a whole, i.e. NPF but also growth of pre-existing particles, as mentioned in Section 3.3.2: *"On event days, the diurnal variation of N_{50} was strengthened due to the concurrent formation of <u>secondary aerosols, i.e. including the formation and growth of new particles as well as the growth of pre-existing larger particles</u> mentioned earlier (Fig. 9.d)"*, *"Following these hypotheses, the contribution of <u>secondary aerosols</u> to the observed CCN population was estimated from the difference between the median of the N_{50} absolute increase observed on event days (i.e. resulting from transport of particles from the boundary layer and <u>secondary aerosol formation</u>) and that of non-event days (resulting from transport only)".*

(C) It is true that we report higher particle and CCN concentrations in plume conditions compared to non-plume days. However we do not relate those to increased particle growth rates, but rather to increased particle formation rates and to the presence of additional primary particles from volcanic origin during eruptive periods. This is for instance illustrated in the paragraph below, taken from Section 3.3.1: *"This observation was consistent with the <u>enhanced production of particles</u> previously reported for lower sizes in plume conditions, as the increase of the particles concentration in the Aitken mode most likely resulted from the growth of smaller particles originating from the nucleation mode. As already mentioned, the concentrations of the 2 accumulation modes measured at 07:00 LT were both significantly higher on plume days (235 4800 and 100 1300 cm-3, for the first and second accumulation mode, respectively) compared to non-plume days (80 and 18 cm-3, respectively), most likely due to <u>additional sources of particles at the vent of the volcano during eruptive periods</u> (see Section 3.2.1)".*
Nonetheless it is true that the sentence at the end of Section 3.3.2 was confusing, and was thus slightly modified for clarity: *"the growth of ~~the newly formed~~ <u>more</u> particles to CCN relevant sizes was favoured during NPF events occurring in the presence of large amount of H2SO4 caused by the eruptions".*

Minor/technical issues

Comment 1: Page 7, line 4: "...when global radiation >50 ...". Something is missing from here (was?).

5   **Reply 1**: "was" added.

Comment 2: The format of providing the time difference (i.e. 2h10) in section 3.1.2 seems strange to me. Is this a correct way of expressing the time difference?

10   **Reply 2**: We are actually not sure about the expected format for expressing a time difference; we anyway changed it to "XX hours and YY minutes" instead of "XXhYY".

Comment 3: Page 10, line 2: "GR12-19 showed an important variability, ...". What do the authors mean by "important" here?

15   **Reply 3**: The "important" variability was related to the inter-quartile range; this aspect is now better addressed: "*GR_{12-19} showed an important variability, as reflected by the monthly inter-quartile ranges, which were on average of the order of 80% of the corresponding medians*".

Comment 4: Excluding the last paragraph of section 4, the text in that section mainly summarizes the results discussed earlier
20   in the paper. As a results, an appropriate title of this section would be "4. Summary and Conclusions".

Reply 4: Changed.

Comment 5: Would it be possible to change the lines and marks with yellow color in Figures into some other, more easily
25   visible color?

Reply 5: The number of figures with yellow lines and/or markers is now limited in the revised version of the manuscript, since, after considering comments from Referee #1, strong-plume events are no longer highlighted in Section 3.3. For simplicity, and in order to optimize both the visibility and the contrast with other colours, we have decided to keep yellow in our colour code.
30   However, we were able to improve Fig. 8 (yellow changed into purple), Fig. 7 (yellow changed into green) and Fig. 4.a (yellow numbers into black).

New particle formation in the ~~active~~ volcanic eruption plume of the Piton de la Fournaise: specific features from a long-term dataset

Clémence Rose[1], Brice Foucart[2], David Picard[1], Aurélie Colomb[1], Jean-Marc Metzger[3], Pierre Tulet[2], Karine Sellegri[1]

[1]Laboratoire de Météorologie Physique (LaMP-UMR 6016, CNRS, Université Clermont Auvergne), 63178, Aubière, France.
[2]Laboratoire de l'Atmosphère et des Cyclones (LACy-UMR 8015, CNRS, Université de La Réunion, Météo France), 97744 Saint Denis de La Réunion, France.
[3]Observatoire des Sciences de l'Univers de La Réunion, UMS 3365 (CNRS, Université de La Réunion), 97744, Saint Denis de La Réunion, France.

Correspondence to: Clémence Rose (c.rose@opgc.univ-bpclermont.fr) and Karine Sellegri (k.sellegri@opgc.univ-bpclermont.fr)

Abstract

New particle formation (NPF) is a key atmospheric process which may be responsible for a major fraction of the total aerosol number burden at the global scale, including in particular cloud condensation nuclei (CCN). NPF has been observed in various environments around the world, but some specific conditions, such as those encountered in volcanic plumes, remain poorly documented in the literature. Yet, understanding such natural processes is essential to better define preindustrial conditions and their variability in climate model simulations, ~~as those form the baseline to calculate the radiative forcing caused by anthropogenic emissions~~. Here we report observations of NPF performed at the high-altitude observatory of Maïdo (2165 m a.s.l., La Réunion Island) between 1st January and 31st December 2015. During this time period, 3 effusive eruptions of the Piton de la Fournaise, located ~ 39 km away from the station, were observed and documented, resulting in 29 days of measurement in volcanic plume conditions to be compared with 250 "non-plume days". This dataset is, to our knowledge, the largest ever reported for the investigation of NPF in tropospheric volcanic plume conditions, and allowed for the first time a statistical approach to characterize the process and also assess its relevance with respect to non-plume conditions. NPF was observed on 90% of the plume days vs 71% of the non-plume days during the 4 months when the eruptions occurred. The events were on average detected earlier on plume days, most likely benefiting from larger amounts of precursors available at the site prior to nucleation hours ~~compared to non-plume days, during which condensable species were in contrast transported from lower altitude by the mean of convective processes. Surprisingly,~~ The overall effect of the plume conditions on the particle growth rate was limited. However, with the exception of September, particle formation rates were significantly higher on plume days. The signature of the volcanic plume on the aerosol spectra up to d_p = 600 nm was further investigated based on the analysis and fitting of the particle size distributions recorded in ~~the different conditions~~ and off-plume conditions. The spectra recorded prior to nucleation hours, in absence of freshly formed particles, featured a significant contribution of particles likely formed *via* heterogeneous processes at the vent of the volcano (and assimilated to volcanic primary particles) to the

concentrations of the 2 accumulation modes on plume days. Later on in the morning, the concentrations of the nucleation and Aitken modes showed important variations on plume days compared to event days outside of plume conditions. The spectra recorded on event days, in and off-plume conditions, were further used to provide an average size distribution of the particles of volcanic origin, which clearly highlighted the dominant contribution of secondary over primary particles (93%) to the total concentration measured on NPF event days within volcanic plume. In a next step, particular attention was paid to the concentration of particles with $d_p > 50$ nm (N_{50}), used as a proxy for potential CCN population. The contribution of secondary particles to the increase of N_{50} was the most frequent in plume conditions, and the magnitude of the increase was also more important on plume days compared to non-plume days. Last, in order to further evaluate the effect of volcanic plume conditions on the occurrence of NPF, we analysed the variations of the condensation sink (CS) and [H_2SO_4], previously reported to play a key role in the process. Over the investigated months, higher CS (calculated prior to nucleation hours) were observed in plume conditions, and coincided with high SO_2 mixing ratios. Those most likely compensated for the strengthened loss rate of the vapours and favoured the occurrence of NPF, suggesting at the same time a key role of H_2SO_4 in the process. This last hypothesis was further supported by the correlation between the formation rate of 2 nm particles (J_2) and [H_2SO_4], and by the fair approximation of J_2 that was obtained by the mean of a recent parameterisation of the binary nucleation of $H_2SO_4 - H_2O$. This last result was of high interest as it also demonstrated that in absence of direct measurement of [H_2SO_4] and sub-3 nm particles concentration, estimates of J_2 could be obtained from the knowledge of SO_2 mixing ratios only. Finally, the use of the parameterisation also highlighted the contribution of different nucleation pathways, charged and neutral, over the investigated [H_2SO_4] range, with ion induced nucleation dominating cluster formation for [H_2SO_4] below $\sim 8 \times 10^8$ cm^{-3}.

1 Introduction

Aerosol particles are a complex component of the atmospheric system which affects both air quality and climate. They have been the focus of a growing number of studies during the last decades, but our knowledge of their sources, properties, including their ability to interact with other atmospheric components and associated effects on the Earth's climate system, remains nonetheless uncomplete. In specific, while particles are known to affect the formation of clouds, and in turn their properties (Albrecht, 1989; Rosenfeld et al., 2014), the radiative forcing associated to these effects (usually referred to as "indirect effect") is known with a still has a large uncertainty (Myhre et al., 2013). Better understanding and quantification of this indirect effect requires, in particular, more accurate information on secondary aerosol particle sources, and in turn on new particle formation (NPF). Indeed, measurements conducted in various environments suggest that NPF might be an important source of cloud condensation nuclei (CCN) (e.g. Kerminen et al., 2012; Rose et al., 2017), which is further supported by model investigations (Merikanto et al., 2009; Makkonen et al., 2012; Gordon et al., 2017). However, despite significant improvement of instrumental techniques for the characterisation of the newly formed particles and their precursors (Junninen et al., 2010; Vanhanen et al., 2011; Jokinen et al., 2012), model predictions are still affected by our limited understanding of NPF. In addition, the scarcity

of observations makes it all the more uncertain in hard-to-reach environments, or in specific conditions, such as those encountered in volcanic plumes.

Volcanic eruptions are one of the most important natural sources of some specific gases and aerosol particles in the atmosphere. A variety of gaseous species have been identified in volcanic plumes, among which halogens (Aiuppa et al., 2009; Mather, 2015) and sulphur dioxide (SO_2), which can be further oxidized to sulfuric acid (H_2SO_4). SO_2 is released in significant amount, in particular during eruptive periods but also from passive degassing (Andres and Kasgnoc, 1998; Robock, 2000; Tulet et al., 2017), and it was reported that all together, volcanoes contribute significantly to the global sulphur budget, which is otherwise dominated by anthropogenic sources (Penner et al., 2001 and references therein; Seinfield and Pandis, 2006). Volcanic aerosols are injected in the atmosphere both as primary or secondary particles. The former can be fragments of ash which, despite their relatively large sizes (up to few microns) (Robock, 2000), can be transported over long distances in the atmosphere (Hervo et al., 2012). Primary sulphate aerosols of volcanic origin were also evidenced by near source measurements conducted at Masaya volcano by Allen et al. (2002), who were however not able to identify their precise mechanisms of formation. Several pathways were later suggested for the formation of H_2SO_4 at the vent, including catalytic oxidation of SO_2 inside the volcanic dome (Zelenski et al., 2015), high temperature chemistry in the gas phase (Roberts et al., 2019), as well as aqueous production of H_2SO_4 from SO_2 (Tulet et al., 2017). H_2SO_4 produced by the mean of the aforementioned reactions is expected to contribute to the formation and growth of particles in the close vicinity of the volcano, which are in turn assimilated to primary volcanic aerosols. while the latter Secondary particles, on the other hand, result from gas to particle conversion processes, including NPF, that take place outside of the volcanic dome under atmospheric temperature and pressure.

The occurrence of NPF in volcanic plume conditions was suspected to take place in several earlier studies (e.g. Deshler et al., 1992; Robock, 2000; Mauldin et al., 2003), but the first dedicated study was conducted by Boulon et al. (2011), during the eruption of the Eyjafjallajokull which happened in spring 2010. Indeed, using measurements performed at the high-altitude station of puy de Dôme (1465 m a.s.l., France), the authors linked the occurrence of NPF to unusually high levels of H_2SO_4 corresponding to model predictions of the Eyjafjallajokull plume transport to puy de Dôme, and highlighted a remarkably elevated particle formation rate in these conditions. While H_2SO_4 concentrations were derived from a proxy in this last study, Sahyoun et al. (2019) recently reported new evidence and quantification of the NPF process in the passive plumes of Etna and Stromboli, and supported the key role of H_2SO_4 using direct measurement performed with a state-of-the-art mass spectrometer onboard the French research aircraft ATR-42. The rarity of studies dedicated to the observation of NPF in volcanic plume conditions is illustrated by the absence of any related topic in the recent review by Kerminen et al. (2018), despite the need for understanding such natural processes. Indeed, those might have dominated NPF and CCN formation in the pristine preindustrial era, when anthropogenic emissions were much lower. Our incomplete knowledge of the preindustrial conditions is responsible for a significant fraction of the uncertainty on the impact of aerosols on climate, since these conditions form the baseline to calculate the radiative forcing caused by anthropogenic emissions in climate model simulations (Carslaw et al, 2013; Gordon et al, 2016, 2017). In specific, substantial uncertainties in the pre-industrial baseline cloud radiative state related to the activity of continuously degassing volcanoes were reported by Schmidt et al. (2012).

Despite providing new and highly valuable information, the studies by Boulon et al. (2011) and Sahyoun et al. (2019) however had some limitations. Indeed, they were both based on short datasets, which did not allow for any statistical approach to evaluate the relevance of the process nor proper comparison with the occurrence of NPF outside of plume conditions. Also, airborne measurements conducted in the close vicinity of Etna and Stromboli allowed Sahyoun et al. (2019) to investigate the presence of the newly formed particles soon after the emission of their precursors from the vent of the volcanoes up to few tens of kilometres. They were however unfortunately not able to document properly the evolution of the particle size distribution along the volcanic plumes, but analysed instead the particle concentration in relatively broad size ranges (2.5 – 10 nm, 10 – 250 nm). In addition, as mentioned earlier, this study was focussed on passive plumes, i.e. in the presence of a limited concurrent emission of primary particles by the volcanoes. Conducting similar investigation of ~~active~~ volcanic eruption plumes is by the way more difficult due to the unexpected aspect of active eruptions. Taking the advantage of ground-based measurements and broader instrumental setup, Boulon et al. (2011) were in contrast able to study the time variation of the particle size distribution between 2 nm and 20 µm, and, in turn, to evaluate the strength of the reported NPF events in terms of particle formation and growth rates. Measurements were however conducted after the ~~active~~ volcanic eruption plume of Eyjafjallajokull had travelled several thousands of kilometres, and most likely underwent significant modifications due to the occurrence of chemical processes and dilution during transport.

In this context, the objectives of the present work were to provide new observations of NPF in a~~n active~~ volcanic eruption plume with detailed analysis of the event characteristics, including the capacity of the newly formed particles to reach CCN sizes, and to assess the relevance of the process with respect to non-plume conditions. For that purpose, we used measurements of the particle number size distribution and SO_2 mixing ratios conducted at the Maïdo observatory (2165 m a.s.l., La Réunion Island, Baray et al., 2013) between January 1st and December 31st 2015. During this period, 3 eruptions of the Piton de la Fournaise, which is located in the south-eastern sector of the island (see Fig. 1.a from Tulet et al., 2017), were observed and documented, resulting in 29 days of measurement in plume conditions that could be compared with 250 "non-plume days". This dataset is, to our knowledge, the largest ever reported for the investigation of NPF in volcanic plume conditions.

2. Measurements and methods

2.1 Measurements

Measurements were performed at the Maïdo observatory located on La Réunion Island, in the Indian Ocean (21.080° S, 55.383° E) between January 1st and December 31st 2015. This high-altitude station (2165 m a.s.l.) is surrounded by lush tropical vegetation on the east side (natural amphitheatre of Mafate) and highland tamarin forest on the west side, which dominates the coast where the nearest urban areas of Saint Paul and Le Port are located (105 000 and 40 000 inhabitants, 13 and 15 km away from the station, respectively). The observatory was built in 2012, and since then it has been progressively equipped with a growing instrumental setup dedicated to the monitoring of the upper troposphere and the lower stratosphere, including both in-situ and remote sensing techniques. Measurements conducted at Maïdo are of great interest since the observatory is one of

the very few multi-instrumented stations in the tropics, and more particularly in the Southern hemisphere. Evidence of this is the involvement of the station in several international networks such as NDACC (Network for the Detection of Atmospheric Composition Change) and ACTRIS (Aerosol Cloud and Trace gases Research Infrastructure), and in the GAW (Global Atmospheric Watch) regional network, which all ensure the quality of the data collected at this site. In addition, the proximity

5   of the Piton de la Fournaise, located in the south-eastern region of the island ~ 39 km away from Maïdo, gives a strategic position to the station for the particular investigation of volcanic plume conditions, which are in the scope of the present work. More detailed information about the facility can be found in Baray et al. (2013) and Foucart et al. (2018), including a description of the large and local scale atmospheric dynamics which affect the observations performed at the site. An overview of the monitoring of the volcanic plume performed at Maïdo during the eruptions of the Piton de la Fournaise observed in 2015

10 is in addition available in Tulet et al. (2017).

The instrumental setup used in the present work was previously described in the companion study by Foucart et al. (2018). The aerosol size distribution between 10 and 600 nm was measured with a custom-built Differential Mobility Particle Sizer (DMPS), with a time resolution of 5 min. Particles are first charged to equilibrium using a Ni-63 bipolar charger, after which they enter the DMPS, which includes a TSI-type Differential Mobility Analyzer (DMA) operating in a closed loop and a

15 Condensation Particle Counter model TSI 3010. The instrument was operated behind a Whole Air Inlet (higher size cut-off of 25 μm for an average wind speed of 4 m s^{-1}), and measurement protocols were defined with respect to the ACTRIS recommendations regarding both the flow rates and RH (Wiedensohler et al., 2012). The particle size distributions measured with the DMPS were used to detect the occurrence of NPF and to calculate the event characteristics, such as the particle formation and growth rates (see Sect. 2.2), and to further evaluate the potential of the newly formed particles to reach CCN

20 relevant sizes. DMPS data was also used to calculate the condensation sink (CS), which describes the loss rate of gaseous precursors on pre-existing particles (Kulmala et al., 2012). In addition to DMPS, an Air Ion Spectrometer (Airel, Estonia, Mirme et al., 2007) was operated at Maïdo between May and October 2015. The AIS includes two DMA which allow simultaneous detection of negative and positive ions and charged particles in the mobility range 0.0013-3.2 cm^2 V^{-1} s^{-1}, corresponding to mobility diameter 0.8-42 nm in NTP-conditions (Mäkelä et al., 1996). Each analyser is working with a flow

25 rate of 90 L min^{-1} (sample flow rate of 30 L min^{-1} and sheath flow rate of 60 L min^{-1}) in order to reduce diffusion losses in the instrument, and measurements were conducted through an individual short inlet (30 cm) to further limit the loss of ions in the sampling line. AIS data was collected with a time resolution of 5 min and was analysed in the present work to get further insight into the timing of the early stages of the NPF process.

SO$_2$ mixing ratios used to monitor the occurrence of volcanic plume conditions at Maïdo were measured with a UV

30 fluorescence analyser (Thermo Environmental Instrument TEI 43) operated by ATMO-Réunion (formerly referred to as ORA, Observatoire Réunionnais de l'Air), with a time resolution of 15 min. The detection limit of the instrument was about 0.5 ppb, which is above the usual SO$_2$ mixing ratios encountered at Maïdo outside of the eruptive periods of the Piton de la Fournaise (see Fig. A1 in Foucart et al. 2018).

Finally, meteorological parameters recorded with a time resolution of 3 s were used as ancillary data. Global radiation was measured with a Sunshine Pyranometer (SPN1, Delta-T Dvices Ltd., resolution 0.6 W m^{-2}), and other variables of interest including temperature, wind speed and direction and relative humidity (RH) were recorded using a Vaisala Weather Transmitter WXT510.

5　An overview of the data availability for all abovementioned instruments between January 1st and December 31st 2015 is provided in Foucart et al. (2018, Fig. 2).

2.2 Particle formation and growth rates

As previously reported in Foucart et al. (2018), the formation rate of 12 nm particles (J_{12}) expressed in cm^{-3} s^{-1} was calculated based on DMPS data following Kulmala et al. (2012):

10　$$J_{12} = \frac{dN_{12-19}}{dt} + CoagS_{12} \times N_{12-19} + \frac{GR_{12-19}}{7\,nm} \times N_{12-19} \qquad (1)$$

where N_{12-19} (cm^{-3}) is the number concentration of particles in the diameter range 12-19 nm, $CoagS_{12}$ (s^{-1}) represents the coagulation sink of 12 nm particles on larger particles and GR_{12-19} (nm h^{-1}) is the particle growth rate between 12 and 19 nm. The second and third terms on the right-hand side of Eq. (1) thus represent the loss rate of particles in the range 12-19 nm due to coagulation on pre-existing larger particles and condensational growth outside of the size range, respectively. Together with

15　the production term J_{12}, these loss terms determine the time evolution of the particle concentration in the range 12-19 nm, denoted as $\frac{dN_{12-19}}{dt}$. GR_{12-19} was estimated from DMPS data based on the "Maximum method" introduced by Hirsikko et al. (2005). Briefly, the times t_m when the maximum concentration successively reached each of the DMPS size bins between 12 and 19 nm were first determined by fitting a normal distribution to the concentration time series of each bin. GR_{12-19} was then obtained by fitting a linear least square fit through the t_m values previously identified. Note that the use of $CoagS_{12}$ for all

20　particles in the range between 12 and 19 nm might cause some overestimation of the actual coagulation losses, and in turn lead to high estimates of J_{12}.

In order to get further insight into the early stages of the NPF process, and in absence of direct measurement of sub-3 nm particles, J_{12} and GR_{12-19} were used to derive the formation rate of 2 nm particles (J_2) following the equation from Lehtinen et al. (2007):

25　$$J_2 = \frac{J_{12}}{exp\left(-\gamma \times 2\,nm \times \frac{CoagS_2}{GR12-19}\right)} \qquad (2)$$

where,

$$\gamma = \frac{1}{m+1}\left[\left(\frac{12\,nm}{2\,nm}\right)^{m+1} - 1\right] \qquad (3)$$

and,

$$m = \frac{log(CoagS_{12}) - log(CoagS_{2})}{log(12\ nm) - log(2\ nm)} \tag{4}$$

In Eq. (2) and (4), $CoagS_2$ represents the coagulation sink of 2 nm particles on larger particles. Equation (2) is based on the assumption that the particle growth rate is constant over the range 2 – 19 nm, which is most likely not the case, as particle growth rates are usually reported to increase with particle diameter (Yli-Juuti et al., 2011), including high altitude sites (e.g.

5 Rose et al., 2015). In order to further investigate the effect of the particle growth rate on the prediction of J_2 with Eq. (2), we have performed a sensitivity study. The term $\gamma \times 2\ nm \times CoagS_2$ (hereafter referred to as Fact$_J$) was found to vary between $\sim 5.0 \times 10^{-5}$ and $\sim 1.2 \times 10^{-3}$ nm s^{-1} (10th and 90th percentiles, respectively), and the GR_{12-19} obtained during the events of interest, i.e. observed in May, August, September and October (see Sect 2.3 for more details about the selected period), were found in the range between GR_{low} = 7.8 nm h^{-1} and GR_{high} = 42.7 nm h^{-1} (10th and 90th percentiles, respectively). Considering the

10 abovementioned lower limit of Fact$_J$, varying GR_{12-19} between GR_{low} and GR_{high} did not affect the calculation of J_2, and repeating the same procedure with $GR_{low}/2$ and $GR_{high} \times 2$ lead to the same result. Considering then a case with Fact$_J$ in the high end of observed values, i.e. $\sim 1.2 \times 10^{-3}$ nm s^{-1}, varying GR_{12-19} between GR_{low} and GR_{high} resulted in a factor of ~ 1.6 in the calculation of J_2, and repeating the test with the more extreme values $GR_{low}/2$ and $GR_{high} \times 2$ only increased the factor to ~ 3.0. All in all, this sensitivity study demonstrates that the accuracy of the particle growth rate only has a limited effect on

15 the calculation of J_2 with Eq. (2) in the conditions of the present analysis.

2.3 Detection of the volcanic plume

Four eruptions of the Piton de la Fournaise were observed in 2015: the first in February, the second in May, the third at the very beginning of August, and, the last, from the end of August to late October. More details about the exact dates and characteristics of the eruptions can be found in Tulet et al. (2017). Figure 1.a presents the timeseries of the SO$_2$ mixing ratio

20 measured at Maïdo between May and December 2015, and highlights as well the eruptive periods of the Piton de la Fournaise observed during this period (Tulet et al., 2017), which logically coincide with the detection of high SO$_2$ levels at the station. More specifically, the Maïdo was considered to be in volcanic plume conditions when at least three of the hourly averages of the SO$_2$ mixing ratio measured between 06:00 and 11:00 LT (UTC +4) were ≥1 ppb, which corresponds to the 97th percentile of SO$_2$ mixing ratio on non-eruptive days. The relatively low SO$_2$ mixing ratios observed outside of the eruptive periods,

25 mostly below the detection limit of the instrument, reflect the low pollution levels characteristic of this insular station, located at high altitude in a region rarely subject to significant influence of pollution from continental origin. The specific time period between 06:00 and 11:00 LT was chosen because it includes the usual nucleation hours at the site (see Sect. 3.1.2 and Foucart et al., 2018), as the main purpose of the present work is to evaluate the effect of volcanic plume conditions on NPF. This last criterion classification slightly differs from that introduced earlier by Foucart et al. (2018), who did not restrict the plume

30 detection to morning hours, but focussed instead on daytime values, i.e. when global radiation was > 50 W m^{-2}, and required only one hourly average of the SO$_2$ mixing ratio ≥1 ppb to assess the occurrence of plume conditions. Also, in order to avoid

any misclassification of the days, all data between 4th and 17th of February were excluded from the analysis, since the lack of SO$_2$ measurement prevented from a proper identification of the plume conditions at Maïdo during this eruptive period. Consequently, only the last three eruptions of the year 2015, which occurred in May and over the period August-October, are discussed in the present work.

5   In total, 30 days were classified as "plume days" following the abovementioned criteria, among which 1 was excluded from further analysis due to DMPS malfunctioning. All these 29 days were previously classified as plume days by Foucart et al. (2018), who identified in total 44 plume days with available DMPS measurement. The difference in the classifications arises from the different time windows investigated in the two studies, i.e. morning nucleation hours (this study) vs daytime (Foucart et al., 2018), and from the criterion on the number of hourly averages of the SO2 mixing ratio ≥1 ppb needed for the plume

10   detection. In fact, plume conditions were detected after 11:00 LT on 8 of the 15 additional plume days reported by Foucart et al. (2018), and the plume conditions lasted during only 1 or 2 hours on the remaining days. The majority of the 29 plume days (22/29) were identified during the longest of the eruptions of the Piton de la Fournaise observed in 2015, which occurred between end of August and late October. Six of the remaining plume days were detected in May, and the last day was identified during the very short eruption observed in late July – early August. In the end, after filtering the data for instrument

15   malfunctioning and / or absence of measurements (71 days in total), 29 plume days and 250 non-plume days were included in the analysis. The 15 remaining days, with late or short plume occurrence, will ~~not be further~~ only be shortly discussed in Section 3.1.1.

   In addition to the abovementioned classification, we further analysed the characteristics of the plume days in terms of 1) the duration of the plume conditions detected at Maïdo (from 3 to 5 hours between 06:00 and 11:00 LT) and 2) the level of the

20   hourly average SO$_2$ mixing ratios measured during the same time period. The plume was detected during the 5 hours of the time window of interest on 20 of the 29 days, and during 4 and 3 hours on 5 and 4 days, respectively. ~~More sporadic appearance of plume conditions during 1 or 2 hours were only observed on 7 days, indicating that 80% of the plume days were characterized by plume conditions lasting during at least 3 hours between 06:00 and 11:00 LT.~~ Concerning the SO$_2$ levels, they varied significantly from day to day. As an indicator of the "strength" of the plume, we calculated for each plume day the

25   median of the SO$_2$ hourly averages ≥1 ppb identified between 06:00 and 11:00 LT. For 6 of the 29 plume days, the median SO$_2$ level was found between 1 and 2 ppb, and 17 days showed median levels relatively homogeneously distributed in the range between 2 and 14 ppb. Higher median SO$_2$ mixing ratios were observed on the remaining days, up to 249 ppb on the 20th of May. Based on this analysis, and in order to evaluate more specifically the effect of "strong" plume conditions on NPF (regarding both the duration of the plume conditions and the magnitude of the SO$_2$ levels), we further defined a sub-class of

30   plume days, hereafter referred to as "strong plume days". The strong plume days were defined as plume days for which 1) the plume conditions lasted from 06:00 to 11:00 LT, with 2) the median of the SO$_2$ hourly averages ≥ 5 ppb. In total, 14 days were classified as strong plume days based on these criteria. Note that these days were included in the statistics reported for plume days in the next sections, and were in addition highlighted separately. The threshold of 5 ppb was chosen as it led to a fair compromise between the number of days to be classified as strong plume days, which we wanted to keep significant for the

relevance of our analysis, and a mixing ratio of SO_2 significantly higher than that measured during non-eruptive periods. For comparison, 5 ppb corresponds to intermediate mixing ratios reported for polluted megacities (Mallik et al., 2014). As an illustration, Fig 1.b and c present the negative ion and particle number size distributions measured on two NPF event days detected during the eruptive period in May, in regular (May 29th) and strong (May 21st) plume conditions, respectively.

2.4 Sulfuric acid concentration in the gas phase

In the absence of direct measurements, we used a proxy to estimate the concentration of gaseous sulfuric acid. To our knowledge, there is no specific proxy dedicated to the rather unusual volcanic plume conditions, so we considered instead the expressions from Petäjä et al. (2009) and Mikkonen et al. (2011), which have already been widely used in nucleation studies. The two proxies have the common feature to consider the oxidation of SO_2 by OH as the only source of H_2SO_4, and do not include the contribution of other oxidants possibly emitted together with SO_2 in the volcanic plume, and possibly prone to contribute to H_2SO_4 production, as discussed earlier by Berresheim et al. (2014) for the coastal atmosphere. The two proxies however differ in their construction, as Petäjä et al. (2009) used data collected solely in the boreal forest, while Mikkonen et al. (2011) used measurements from different locations, including the urban area of Atlanta, where, to a certain extent, SO_2 mixing ratios are resembling those measured at Maïdo in plume conditions. Besides the variety of measurement conditions, the expression from Mikkonen et al. (2011) also considers more parameters, including the temperature dependant reaction rate between SO_2 and OH as well as the relative humidity, which can fluctuate a lot and reach high values at mountain sites such as Maïdo. Given the above, the proxy developed by Mikkonen et al. (2011) was finally used in the present work. However, since the relevance of this proxy could not be evaluated in volcanic eruption plume conditions, neither from available measurements nor existing literature, one should keep in mind the potential limits of using such parametrization when interpreting the related results.

3. Results

3.1 NPF analysis in the volcanic plume

3.1.1 Frequency of occurrence

As mentioned in Sect. 2.3, 29 plume days were identified at Maïdo as a consequence of the 3 eruptions of the Piton de la Fournaise which could be documented in 2015. Besides the plume days, 250 days with no influence of the volcanic plume were identified and included in the analysis (days with plume conditions detected in the afternoon or short plume occurrence were excluded, 15 days in total, see Sect. 2.3 for more details); these days will be hereafter referred to as "non-plume days". Figure 2 shows the monthly NPF frequency separately for plume and non-plume days, with a specific focus on May, August, September and October 2015, when the eruptions were observed. Note that statistics for non-plume days were previously reported for all months in 2015 by Foucart et al. (2018). Our results suggest that volcanic plume conditions favour the

occurrence of NPF at Maïdo since all the plume days were classified as NPF event days with the exception of 3 days classified as undefined in September, leading to higher NPF frequencies in plume conditions compared to non-plume days over the months highlighted on Fig. 2 (90% vs 71%). Focussing on the strong plume days, 12 were classified as event days and the remaining 2 days were classified as undefined. At the annual scale, i.e. when including all months in the calculation, the NPF

5   frequency was raised from the already remarkably high value of 67% when excluding the plume days to 69% when considering both plume and non-plume days. Such values are among the highest in the literature, similar to those previously reported for the high-altitude station of Chacaltaya (5240 m a.s.l., Bolivia) (64%, Rose et al., 2015) and the South African savannah (69%, Vakkari et al., 2011), slightly lower compared to that reported for the South African plateau, where NPF events are observed on 86% of the days (Hirsikko et al., 2012).

10 In addition, a quick analysis was also performed on the 8 days for which the volcanic plume was detected after the morning hours during which nucleation is usually initiated (see Sect. 3.1.2 for more details about the timing of NPF). With the exception of one day classified as undefined in October, all other days were classified as NPF event days, but there was no clear evidence of an effect of the "late" plume conditions on the ongoing events, triggered earlier during the day. High SO_2 mixing ratios (up to several hundreds of ppb) associated to plume conditions were also measured during the night, but they were not accompanied

15 by any obvious particle formation nor growth process at Maïdo, supporting a determinant role of photochemistry in these secondary particle formation processes.

3.1.2 Timing of the events

As a first investigation of the specificities of NPF in plume conditions, we performed a simple analysis of the starting time of the NPF events on plume and non-plume days. The starting time of an event was defined by a visual inspection as the time

20 when the 1.5-2.5 nm ions concentration measured with the AIS significantly increased. Only the events simultaneously detected with the AIS and the DMPS were included in this analysis, and the dataset was not limited to May-August-September-October, but included instead all available AIS data between mid-May and end of October. In total, 36 events observed on non-plume days and 10 events detected in plume conditions were documented.

The median starting time of NPF in non-plume conditions was found at 08:36 LT [25th percentile: 08:15 LT; 75th percentile:

25 09:06 LT]. Earlier rising time of the cluster concentration was observed on plume days, around 07:41 LT [07:18 LT; 08:16 LT]. In addition, we also calculated the median time laps between sunrise and beginning of NPF, since the starting time of NPF was most likely affected by the change in sunrise time over the course of the investigated period. Median time laps between sunrise and rising time of the cluster concentration was 2 hours and 11 minutes [1 hour and 55 minutes; 2 hours and 26 minutes] on non-plume days, with a minimum of 54 min observed on May 18th, and was about ~~half an hour~~ 45 minutes

30 shorter in plume conditions, being 1 hour and 26 minutes [57 minutes; 1 hour and 38 minutes], with a minimum of 29 min obtained on August 28th. These observations suggest that on plume days, when precursors related to volcanic plume conditions were available prior to sunrise in a sufficient amount, photochemistry was the limiting factor for NPF to be triggered. In contrast, on non-plume days, NPF was certainly limited by the availability of condensable species, which were most likely

transported from lower altitude by the mean of convective processes taking place after sunrise. Further discussion on the precursors involved in the process is reported in Sect. 3.2.2.

3.1.3 Particle formation and growth rates

Figure 3 shows the formation rate of 2 and 12 nm particles (J_2 and J_{12}, respectively), as well as the particle growth rate between 12 and 19 nm (GR_{12-19}). Note that statistics reported for plume days do include data from the strong plume days, which are in addition highlighted separately. Besides the high values observed on some of the strong plume days, which exceed those measured on regular plume days, GR_{12-19} showed an important variability, as reflected by the monthly inter-quartile ranges, which were on average of the order of 80% of the corresponding medians. Also, with the exception of May, the monthly medians of GR_{12-19} were higher on non-plume days compared to plume days (Fig. 3.a). The overall effect of the plume conditions on the particle growth thus appeared to be limited. This observation is most likely related to the fact that not only the amount of precursor vapours (including for instance SO_2, see Fig. 1.a) was increased in the volcanic plume, but also the number concentration of the particles to grow, from both primary and secondary origin, as also reflected in the variations of the CS (Sect. 3.2.1) and discussed later in Sect. 3.3.1.

In contrast, the effect of plume conditions was more pronounced on the particle formation rates, both for J_2 and J_{12} (Fig. 3.b and c). Indeed, with the exception of September, when ~~comparable~~ slightly lower median values were found in plume conditions, the particle formation rates were on average increased on plume days, with the most important difference observed in May, when median J_2 and J_{12} were increased by a factor of ~ 17 and 7.5, respectively, in plume conditions. However, most of the values obtained on strong plume days were similar to those measured during regular plume days of the same month. Higher particle formation rates observed on plume days indicate that particles were constantly formed in the volcanic plume along the transport pathway to Maïdo, showing that nucleation and growth taking place over a distance of the order of 40 km appears like a regional scale homogeneous process, which can be described with the usual equations (Eq. 1-4) recalled in Sect. 2.2. A rough estimate for the transport time of the particles nucleated in the vicinity of the volcano to the Maïdo observatory can be obtained by dividing the distance between the sites by the median wind speed measured on NPF event days: 39 km ÷ 1.8 m s^{-1} ≈ 6 hours. This indicates that in such conditions, the GR_{12-19} reported on Fig. 3.a were often sufficient (> 8 nm h^{-1}) for the newly formed particles (~ 1 nm) to grow up to CCN relevant sizes (~ 50 nm, see Sect. 3.3.2) during their transport, further explaining the observation of the typical banana shape of the events, both on plume and non-plume days. Similar analysis was repeated with the 75th percentile of the wind speed measured on NPF event days (2.9 m s^{-1}), and, again, the observed growth was often fast enough (> 13 nm h^{-1}) for the particles to reach 50 nm during the corresponding ~ 3 hours 45 minutes trip to Maïdo.

These observations suggest that, despite a limited effect on particle growth, plume conditions do affect NPF, both in terms of frequency of occurrence and particle formation rate. However, assessing the real effect of these specific conditions on the particle formation and growth is challenging. In specific, as previously highlighted in the companion study by Foucart et al. (2018), the particle growth rates calculated from high altitude stations such as Maïdo are "apparent" due to the complex

21

atmospheric dynamics around these sites, and may in particular be overestimated due to the concurrent transport of growing particles to the site. Influence of the volcanic plume on larger particles, including CCN relevant sizes, is further investigated in Sect. 3.3., while the next section is focussed on the analysis of key atmospheric components previously reported to influence NPF, both in terms of frequency of occurrence and characteristics.

3.2 Effect of key atmospheric components on the NPF process

NPF has been previously reported to be influenced by various atmospheric parameters, including solar radiation, temperature (Dada et al., 2017), as well as RH, which effect on the process is certainly the less evident to predict and understand (e.g. Birmili et al., 2003; Duplissy et al., 2016). In the frame of the present analysis, the median diurnal variations of the abovementioned parameters reported on Fig. S1 (in the Supplementary) did not highlight any specificity for the events observed on plume days, and displayed similar behaviour in and off-plume conditions.

In addition to the aforementioned meteorological variables, which are thought to influence directly the production of the nucleating and growing vapours as well as the survival of the newly formed clusters, other factors were shown to affect NPF, such as for instance the loss rate of the condensing compounds on pre-existing particles. The effect of the volcanic plume on this last parameter is discussed below, while the role of H_2SO_4, expected to play a determining role in the events observed on plume days (Boulon et al., 2011; Sahyoun et al., 2019), is investigated in the following section.

3.2.1 Condensation sink

As recalled in Sect. 2.1, the condensation sink represents the loss rate of precursor vapours on pre-existing larger particles, and is thus expected to affect directly the amount of precursors available for NPF. In order to further investigate the effect of this parameter on the occurrence of NPF and avoid any interference with the CS increase caused by the newly formed particles themselves, we focus here on the CS observed prior to usual nucleation hours, between 05:00 and 07:00 LT.

Figure 4.a. shows the monthly median of the CS calculated over the abovementioned time period, separately for plume, strong plume and non-plume days, event and non-event days. Note that strong plume days were included in the statistics reported for plume days, and were also highlighted separately. The comparison of non-plume NPF event and non-event days did not highlight any clear tendency over the months of interest for this study. Indeed, comparable median CS were observed in August regardless the occurrence of NPF later during the day, higher values were in contrast obtained on event days in May, while the opposite was observed in September and October, most likely related to biomass burning activity in South Africa and Madagascar during austral spring (Clain et al., 2009; Duflot et al., 2010; Vigouroux et al., 2012). The overall number of non-event days included in the statistics was however limited, and using comparable time window Foucart et al. (2018) reported that CS was on average higher on NPF event days compared to non-event days when including all the data from 2015. These contrasting results are representative of the observations from high altitude observatories at a larger scale, where both the location of the sites, their topography and the fast changing conditions related to complex atmospheric dynamics are likely to influence the effect of the CS on the occurrence of NPF. Indeed, Boulon et al. (2010) and Rose et al. (2015) reported that CS

was on average positively correlated with the occurrence of NPF at Jungfraujoch (3580 m a.s.l., Switzerland) and Chacaltaya, respectively. These observations suggest that the availability of the precursors was often limiting the process at these sites, which seemed to be fed with vapours transported together with pre-existing particles contributing to the CS. In contrast, the CS was observed to be on average lower on NPF event days compared to non-event days at puy de Dôme, which could be in a less precursor-limited environment due to its lower altitude (Boulon et al., 2011).

Despite an important variability of the reported values, the median CS obtained on plume days were on average higher than those observed on non-plume days, with the largest difference in May. The CS reported for strong plume days were even higher, with median values on average increased by one order of magnitude compared to non-plume event days (up to 30 times higher in May). One might have expected those enhanced CS to inhibit NPF at Maido, which was instead more frequent in plume conditions compared to non-plume days (Sect. 3.1.1). This non-intuitive result is most likely explained by the increased mixing ratios of SO_2 (Fig. 4.b), and in turn [H_2SO_4], which were concurrently measured on strong plume days. Assuming that H_2SO_4 was contributing to NPF in such conditions, as previously suggested by Boulon et al. (2011) and Sahyoun et al. (2019), increased SO_2 emissions probably compensated for the strengthened loss rate of the condensing vapours involved in particle formation and growth on plume days, and eventually let NPF occur. In addition, the balance between the amount of SO_2 and the magnitude of the CS most likely influenced the strength of the observed events, and explained in specific the variable trends highlighted earlier in the comparison of the particle formation rates calculated on plume and non-plume days (see Sect. 3.1.3, Fig. 3.b and c). Indeed, as reported previously, the largest CS increase observed between non-plume and plume NPF event days occurred in May, when SO_2 mixing ratios were also the highest (Fig. 1), with a median of 26.7 ppb [25th percentile: 1.1 ppb; 75th percentile: 120.5 ppb] calculated during nucleation hours (06:00 and 11:00 LT). We may thus hypothesize that the resulting conditions were highly favourable to NPF, and not only lead to high NPF frequency (Fig. 2), but also to stronger events, with increased particle formation rates compared to non-plume days (Fig. 3.b and c). In September and October, the median CS measured in plume conditions were comparable to that observed in May (Fig. 4.a), but SO_2 mixing ratios were in contrast lower during nucleation hours, with medians around 3.4 ppb [1.5 ppb; 5.6 ppb] and 3.8 ppb [1.9 ppb; 16.9 ppb], respectively. This most likely resulted in less favourable conditions for NPF than in May, which in turn did not enhance the particle formation rates compared to non-plume days. Higher CS observed on plume days also supported the fact that in plume conditions, as suggested in the previous section, the number of particles to grow was increased compared to non-plume days, and the concurrent strengthening of the precursor source rate was on average not sufficient to result in faster particle growth. Nonetheless, while it was possible to evidence the abovementioned trends with our statistical approach, one should keep in mind that both the occurrence and characteristics of NPF are likely to be affected at very short time scales due to the variable nature of the volcanic eruptions. Deeper investigation of the effect of the volcanic eruption plume on NPF would thus require more detailed analysis of the event to event variability, which was however beyond the scope of the present work. The involvement of H_2SO_4 in the NPF process is further investigated in the next section.

The origin of the particles responsible for increased CS prior to nucleation hours on plume event days remains uncertain, but the high SO_2 mixing ratios which were measured concurrently suggest a volcanic origin for these accumulation mode particles

(see Sect. 3.3.1 for more details about the shape of the particle number size distribution). The presence of accumulation mode particles emitted as primary ash have seldomly been reported in the literature, as the instrumentation used for volcanic studies is not adapted for measuring such small sizes. In the case of the Piton de la Fournaise, the existence of such particles was however very unlikely. Indeed, this basaltic volcano was reported to only emit negligible amount of ash, which were observed in the form of Pele's hairs during very specific eruptions (Di Muro et al., 2015); if present, we would have expected the fragments of ash to also cause an increase of the particle mass in the coarse mode, which was not obvious during the eruptions observed in 2015 (Tulet et al., 2017). Other nocturnal sources of aerosols at the vent of the volcano and transport of these particles to Maïdo were in contrast more probable. A first possible production pathway is related to the fact that the Piton de la Fournaise is characterized by an usual water loading, reflected by high H_2O/SO_2 ratios (Tulet et al., 2017). In specific, there is continuous formation of liquid water at the vent of the volcano; gaseous SO_2 can thus be dissolved into the droplets, leading to aqueous formation of H_2SO_4, which likely further condense onto pre-existing particles after evaporation of the cloud in the vicinity of the Piton de la Fournaise (Tulet et al., 2017). Catalytic oxidation of SO_2 inside the volcanic dome was also reported as a potential source of H_2SO_4 by Zelenski et al. (2015) based on measurements conducted at Bezymianny volcano. Finally, Roberts et al. (2019) recently suggested high temperature chemistry as a source of H_2SO_4 precursors in the near-source volcanic plume using model simulations. ~~Finally, heterogenous formation of H_2SO_4 from H_2S occurring at the vent of the volcano, at high temperature, might also contribute to the observed particle loading~~. The abovementioned particles, originally formed or transformed *via* heterogeneous mechanisms occurring in the very close vicinity of the vent, will be, despite the transformations they probably further undergo during their transport, referred to as volcanic primary particles hereafter, as opposed to secondary particles resulting from gas to particle conversion processes that take place further from the volcanic dome. This nomenclature is consistent with earlier results from Allen et al. (2002), who reported the presence of primary sulphate aerosols at Masaya volcano. These so-called primary particles are also likely to participate in daytime particle concentration, together with photochemically-driven secondary formation pathways.

3.2.2 The role of sulfuric acid

As previously mentioned in Sect. 2.4, sulfuric acid concentrations were obtained from SO_2 mixing ratios using the proxy by Mikkonen et al. (2011). H_2SO_4 has often been reported to play a key role in the early stage of atmospheric NPF (Sipilä et al., 2010; Kulmala et al., 2013; Yan et al. 2018), and in particular in sulphur-rich volcanic plume conditions (Mauldin et al., 2003; Boulon et al., 2011; Sahyoun et al., 2019), thus motivating our specific interest in this study.

Figure 5.a shows all J_2 derived during the NPF events detected in plume conditions as a function of $[H_2SO_4]$. Highest $[H_2SO_4]$ were mostly observed on strong plume days and coincided with the highest J_2, but overall, the relationship between J_2 and $[H_2SO_4]$ did not appear to be significantly different on strong plume days compared to regular plume conditions. In order to further investigate the ~~relationship~~ connection between the cluster particle formation rate and the abundance of H_2SO_4, J_2 was fitted with a simple power model $J_2 = k \times [H_2SO_4]^a$, in a similar way as previously done in earlier studies (Kulmala et al., 2006; Sihto et al., 2006; Kuang et al., 2008; Sahyoun et al., 2019). When considering all data in the fitting procedure, i.e.

including strong plume days, parameters k and a were found to be 1.14×10^{-10} and 1.16, respectively. ~~When focussing on strong plume days only, slightly different fitting parameters were obtained, being 4.47×10^{-18} and 1.97 for k and a, respectively. In both cases~~ The correlation between J_2 and [H$_2$SO$_4$] was moderate~~, especially when limiting the analysis to strong plume days~~ (R² = 0.23) ~~and 0.11, for all plume days and strong plume days only, respectively)~~, but ~~still~~ significant, as indicated by the corresponding p-value (p = 2.35×10^{-24} ~~and 0.01, for all plume days and strong plume days only, respectively~~). As a reminder, the p-value is commonly used to quantify the statistical significance, and indicates in the context of this study the maximum probability for the correlation observed between J_2 and [H$_2$SO$_4$] to result from a coincidence. ~~Our results suggest that different mechanisms were likely to explain the observed formation rates across the investigated [H$_2$SO$_4$] range, with stronger dependence on [H$_2$SO$_4$] above 5×10^8 cm^{-3} observed on strong plume days, as one might have expected. Further investigation of this aspect and comparison with non-plume days was unfortunately not possible since SO$_2$ mixing ratios were mostly below the detection limit of the instrument outside of the eruptive periods of the Piton de la Fournaise.~~

The values calculated for k and a ~~using all data (i.e. including strong and regular plume days)~~ were slightly different from those reported by Kuang et al. (2008) for a set of 7 stations, including 2 insular marine sites in the Pacific Ocean and 5 urban or rural continental sites located in Northern America and Europe, where the authors systematically found a in the range 1.98-2.04 and k between ~ 10^{-14} and 10^{-11}. These values were however calculated from a limited number of events for each site (from 1 to 9 events per site), and were derived from the correlation between J_1 (instead of J_2 in the present work) and measured [H$_2$SO$_4$] (instead of proxy-derived in ours study). Also, none of the NPF events investigated by Kuang et al. (2008) occurred in volcanic plume conditions. Overall, the values derived on plume days at Maïdo were in contrast more consistent with those recently reported by Sahyoun et al. (2019) based on aircraft measurements conducted in the passive plume of Etna (k = 1.84 ×10^{-8}, a = 1.12), despite slight differences in the analysis. Indeed, Sahyoun et al. (2019) used direct measurements of [H$_2$SO$_4$] and investigated the link between [H$_2$SO$_4$] and $J_{2.5}$ instead of J_2. Also, instead of fitting all derived $J_{2.5}$, the dataset was first binned with respect to [H$_2$SO$_4$] (bins of equal length, 0.25×10^8 cm^{-3}), after which median $J_{2.5}$ were calculated for each bin and finally fitted using a power model. As a sensitivity study, and in order to provide a more consistent comparison with the results reported by Sahyoun et al. (2019), we applied similar fitting method; only difference was in the binning procedure, as we used bins with an equal number of data points instead of equal length. The results of this analysis are shown on Fig. S2, in the Supplementary. Applying the fit on median J_2 led to comparable fitting parameters (k = 4.36 ×10^{-10}, a = 1.09), but the resulting correlation between J_2 and [H$_2$SO$_4$] appeared to be significantly stronger (R² = 0.88, p = 5.59×10^{-5}). We also investigated the impact of the number of bins on the final parameters and goodness of the fit (Table S1 in the Supplementary), but varying the number of bins between 10 and 30 did not led to major differences.

In order to get further insight into the nucleation mechanism likely to explain the observed events, we additionally compared the formation rates derived from DMPS measurements with that predicted by the recent parameterization developed by Määttänen et al. (2018), which describes neutral and ion-induced binary nucleation of H$_2$SO$_4$-H$_2$O. We used the Fortran code included in the supplementary electronic material of the paper, and, in a first approach, we run the model using the average of

the temperature, relative humidity and CS calculated during nucleation hours on plume event days. We used an average value of 3 cm⁻³ s⁻¹ for the ion pair production rate, consistent with previously reported values from different sites, including the high-altitude station of puy de Dôme (Rose et al. 2013 and references therein). Otherwise, all settings and parameters were those set by default in the Fortran code. As evidenced on Fig. 5.a, the total formation rate of 2 nm-clusters was mostly explained by ion induced nucleation for $[H_2SO_4]$ below ~ 8×10^8 cm⁻³, while neutral pathways seemed to explain the observations at larger sulfuric acid concentrations.

Deeper analysis of the contribution of binary nucleation to the observed events was then performed, and for that purpose the model by Määttänen et al. (2018) was run for each NPF event, with the corresponding temperature, relative humidity and CS levels. Figure 5.b shows, for the same dataset as in Fig. 5.a, the ratio between J_2 derived from DMPS measurements (referred to as J_{meas}) and J_2 predicted by the parameterization (referred to as J_{param}), which included both neutral and ion-induced nucleation pathways. In addition, we also binned the data with respect to $[H_2SO_4]$ (10 bins with equal number of points) and calculated the median ratio J_{meas}/J_{param} in each bin. As evidenced on Fig. 5.b, 64% of the calculated ratios were < 1, which was unexpected since particle formation rates resulting from the binary nucleation of H_2SO_4-H_2O should not exceed J_{meas}. This result was most likely related to 1) the use of proxy-derived $[H_2SO_4]$ in the calculation of J_{param} and 2) the fact that J_{meas} was not derived from direct measurement of 2 nm particles but from J_{12} and GR_{12-19}, which might have led to additional uncertainty. However, despite this inconsistency, Fig. 5.b illustrates our ability to predict J_2 from SO_2 mixing levels with a relatively fair accuracy, especially for $[H_2SO_4]$ in the range between 1.5×10^8 and 7×10^8 cm⁻³. Indeed, the medians of J_{meas}/J_{param} highlighted on Fig. 5.b indicates that J_{param} was on average within a factor of ~ 3 of J_{meas} for $[H_2SO_4] < 10^9$ cm⁻³. Higher discrepancies were in contrast observed for $[H_2SO_4] > 10^9$ cm⁻³, which may stem from a reduced predictive ability of the proxy by Mikkonen et al. (2011) for the highest SO_2 mixing ratios, since such values were not used in the construction of the proxy, or from the binary nucleation parameterization not being fully adapted to the volcanic plume environment. Nonetheless, despite the abovementioned limits, we believe that the last results are of high interest, because they show that in absence of direct measurement of $[H_2SO_4]$ and sub-3 nm particles concentration, the knowledge of SO_2 mixing ratios can lead to a fair approximation of J_2.

All together, these results suggest that higher SO_2 mixing ratios observed on plume days did contribute to the NPF events observed in such conditions, in agreement with earlier results from Boulon et al. (2011) and Sahyoun et al. (2019). However, the contribution of other compounds to the process could not be excluded based on the available dataset, and additional measurements would be needed to further investigate this aspect, including in specific direct measurement of the chemical composition of the clusters as well as their precursors. Such measurements would also allow more detailed evaluation of the proxy by Mikkonen et al. (2011) for the prediction of $[H_2SO_4]$ in volcanic eruption plume conditions.

3.3 Particle growth up to climate relevant sizes in the volcanic plume

The previous section was dedicated to the analysis of NPF occurrence and characteristics in volcanic plume conditions. In this section, we further investigate the effect of such process on the shape of the particle size distribution, first including all sizes between 10 and 600 nm, and then focussing more specifically on large-enough particles to act as CCN. Since the results we have reported so far only revealed limited signature of strong plume conditions on NPF characteristics, we will no longer put any specific focus on these particular days in this last section. They will however still be included in the statistics reported for plume days.

3.3.1 General features of aerosol particle size distributions

The effect of NPF and/or plume conditions on the particle number size distribution was investigated based on the hourly median particle spectra measured with the DMPS in different conditions between 07:00 and 16:00 LT (Fig. 6). This time period was selected as, besides usual NPF hours, it also includes one hour prior to nucleation hours, which allowed to study the main features of the particle size distribution in the different conditions (plume and non-plume) without fresh influence of NPF, as well as several hours to investigate the change of the spectra caused by particle growth processes. Note that in order to increase the statistical relevance of the results (especially for non-event days), the analysis was not restricted to May-August-September-October, and all available data was included in the analysis. All median spectra were in addition fitted with four Gaussian modes, including nucleation, Aitken and 2 accumulation modes, which parameters are shown on Fig. 7 and also reported in Table A1 of the Appendix. ~~The spectra measured on strong plume days were included in the statistics reported for plume days and are also displayed separately on Fig. 6, but were however not independently fitted with Gaussian modes. Indeed, the uncertainty related to this procedure (and thus on the mode parameters themselves) was significantly increased because of 1) the limited number of days and 2) the important variability of the atmospheric conditions during these specific days.~~

As previously mentioned, the median spectra recorded at 07:00 LT, i.e. prior to nucleation hours, gave a unique opportunity to compare the main features of the particle number size distributions recorded in plume and non-plume conditions in absence of freshly nucleated particles. The spectra measured on non-plume days (both event and non-event days) displayed comparable shapes as well as similar concentrations, while higher concentrations were in contrast measured in plume conditions~~, and more specifically on strong plume days~~. As discussed in Section 3.2.1, these differences, which were the most pronounced for the 2 accumulation modes, were most likely explained by the presence of particles originating from heterogeneous processes occurring at high temperatures at the vent during the eruptive periods, and assimilated to volcanic primary particles. Indeed, in plume conditions the population of the first accumulation mode (modal diameter ~ 100 nm) was on average around 300 cm^{-3}, against 55-80 cm^{-3} on non-plume days, indicating the presence of 220-245 cm^{-3} additional primary particles originating from the volcano on plume days. Following similar reasoning, the contribution of volcanic primary particles to the concentration of the second accumulation mode (modal diameter ~ 190 nm) was around 118-132 cm^{-3}. Hence, there was on average ~~more than~~

27

almost a six-fold increase in the accumulation modes particle number concentration due to the emission of primary volcanic particles. Regarding the diameters of the modes, they did not appear to be significantly affected by the different atmospheric conditions.

Despite some variations of the particle concentration in the different modes, the shape of the spectrum observed at 07:00 LT remained the same throughout the investigated time window on non-event days. The concentrations of the Aitken and first accumulation modes were increased by a factor of ~ 2 between 07:00 LT and 13:00 LT, from 130 to 310 cm^{-3} and 55 to 112 cm^{-3}, respectively, and concurrently the concentration of the second accumulation mode was multiplied by ~ 4, from 32 to 142 cm^{-3}, probably due to the transport of pre-existing particles from lower altitude. Surprisingly, the most important variation was observed for the concentration of the nucleation mode, with a 5-fold increase from 18 to 86 cm^{-3} between 07:00 LT and 12:00 LT despite the absence of NPF. These concentrations were however significantly lower compared to those observed on NPF event days, up to 5700 cm^{-3} in plume conditions. Also, in contrast with NPF event days, the diameters of the modes, including in specific that of the nucleation mode, remained stable throughout the investigated time window (modal diameter ~ 15nm, ~ 36 nm, ~ 83 nm and ~ 164 nm for the nucleation, Aitken, first and second accumulation modes, respectively), indicating the absence of a growth process characteristic of NPF.

Consistent with previous observations reported in Sect. 3.1.2, the starting of NPF was seen at 08:00 LT on event days (regardless the occurrence of plume conditions) from a visual analysis of the spectra, and was further confirmed by the increase of the particle concentration in the nucleation mode, which lasted until 11:00 LT. The most significant change was observed in plume conditions, with a thousand-fold increase of the nucleation mode particle concentration in 4 hours, from 5 to 5700 cm^{-3}, i.e. two orders of magnitude stronger than that observed on non-plume days (from 25 to 1700 cm^{-3}), consistent with the higher particle formation rates observed on plume days (see Sect. 3.1.3). After 11:00 LT, the particle concentration in the nucleation mode was observed to decrease, down to 300 cm^{-3} and 990 cm^{-3} at 16:00 LT, on plume and non-plume days, respectively, most likely because of the growth of particles outside of the mode, as well as their loss on larger particles through coagulation processes. Concurrent increase of the modal diameter was also observed between 07:00 and 13:00 LT on plume days, from 12 to 26 nm, and slightly later, between 09:00 and 16:00 LT, on non-plume days, from 10 to 30 nm, further illustrating the simultaneous formation and growth of the particles.

Still focussing on NPF event days, the changes observed in the parameters of the Aitken and 2 accumulation modes were less pronounced than for the nucleation mode. With the exception of the slight difference observed at 07:00 LT, the Aitken mode displayed similar diameters on plume and non-plume days, with only limited variations over the investigated time window, especially on non-plume days (32-45 nm and 38-46.5 nm, on plume and non-plume days, respectively). Also, the initial concentrations of the Aitken mode measured in the different conditions were similar, ~200 cm^{-3}, indicating that no primary particles of this size were produced by the volcano. The initial concentration of the Aitken mode measured in plume conditions was slightly higher than on non-plume days (270 vs 180 cm^{-3}), indicating that, in addition to accumulation mode particle sizes, primary particles as small as ~ 40 nm might have been produced by the volcano. The increase of the particle concentration observed until 13:00-14:00 LT was in contrast also more pronounced on plume days (~ 7-fold increase in plume conditions,

28

up to 1800 cm^{-3}, vs ~ 4-fold increase on non-plume days, up to 750 cm^{-3}), indicating the presence of ~ 1050 cm^{-3} additional particles in the Aitken mode due to the presence of the plume. This observation was consistent with the enhanced production of particles previously reported for lower sizes in plume conditions, as the particles in the Aitken mode most likely resulted from the growth of smaller particles originating from the nucleation mode. As already mentioned, the concentrations of the 2 accumulation modes measured at 07:00 LT were both significantly higher on plume days (300 and 150 cm^{-3}, for the first and second accumulation mode, respectively) compared to non-plume days (80 and 18 cm^{-3}, respectively), most likely due to additional sources of particles at the vent of the volcano during eruptive periods (see Sect. 3.2.1). Later on, the transport of primary particles originating from the urban areas located at lower altitude as well as the growth of the newly formed particles most likely contributed to the concentration increase observed for the accumulation modes during the course of the ~~nucleation period~~ day, up to 770 and 690 cm^{-3}, respectively, on plume days, against 445 and 130 cm^{-3} on non-plume days. With the hypothesis that vertical transport from the boundary layer was the same on plume and non-plume days, we could evaluate that the volcanic plume secondary aerosol formation contributed to ~ 325 cm^{-3} and ~ 560 cm^{-3} in the first and second accumulation modes, respectively. Concerning the diameter of the modes, that of the second accumulation mode showed limited variations on plume days (185-200 nm), being closed to that observed on non-plume days (191 nm). In contrast, the initial diameter of the first accumulation mode was higher on non-plume days (97 vs 81.5 nm) and also showed a more pronounced increase up to 146 nm over the investigated time period.

Altogether, one can infer from these measurements a distribution of the particles of volcanic origin, including the contributions of both primary and secondary aerosols. Following the above analysis, the concentration of the so called volcanic primary particles was calculated for each mode as the difference between the concentrations measured at 07:00 LT on plume and non-plume days, and the values obtained at 07:00 LT in plume conditions were used for the other characteristics of the modes (i.e. sigma and modal diameter). In addition, the concentration of secondary aerosol particles of volcanic origin was calculated for each mode as the difference between the maximum concentrations observed on plume event days and that observed on non-plume event days, which were found between 11:00 and 14:00 LT depending on the modes and conditions; the values obtained at 12:00 LT in plume conditions, when the effect of secondary aerosol formation on the spectrum was on average the most pronounced, were used for the other characteristics of the modes. Resulting aerosol spectrum is reported on Fig. 8, with the detailed contributions of volcanic primary and secondary particles for each mode. Secondary aerosol particles formed due to the presence of the plume contributed 93% of the total concentration observed on plume event days, clearly dominating all the modes but the first accumulation mode, for which the contribution of volcanic primary particles was more significant. The presence of a secondary contribution to the accumulation modes is likely the result of the growth of particles from the Aitken mode, due to the presence of more condensable gases.

3.3.2 Investigation of the formation of potential CCN during NPF events

The increase of potential CCN concentration during NPF was investigated using DMPS measurements, in a similar way as done earlier by Rose et al. (2017) for the high-altitude station of Chacaltaya, following the approach originally developed by

Lihavainen et al. (2003). It is based on the hypothesis that the lower cloud droplet activation diameter d_{act} of aerosol particles is in the range 50 – 150 nm for the typical supersaturations (SS) encountered in natural clouds, including those forming at high altitude (Jurányi et al., 2011; Hammer et al., 2014). For instance, direct CCN measurements conducted at the high altitude station of puy de Dôme with a dedicated chamber (Roberts and Nenes, 2005) showed that particles in the range 50-150 nm

5   were activated at SS 0.24%, also reported to be representative of in-cloud SS at the site (Asmi et al., 2012). Following this basic assumption, the concentration of potential CCN can be assimilated to the particle concentration $N_{>d_{act}}$ measured above any given d_{act} in the range 50 - 150 nm. Sensitivity studies are usually performed using multiple activation diameters, which reflect the effect of both the properties of the particle itself (such as the chemical composition) and atmospheric conditions (such as the supersaturation) on the ability of a particle to activate into a cloud droplet (e.g. Kerminen et al. 2012 and references

10 therein). We used in a first approach the same activation diameters (50, 80 and 100 nm) as Rose et al. (2017), and we based our analysis on both the time series of the concentration of particles larger than these thresholds (hereafter referred to as N_{50}, N_{80} and N_{100}, for 50, 80 and 100 nm, respectively) and the overall shape of the event reflected by the corresponding surface plot. This indirect method based on DMPS measurements only provides estimations of potential CCN concentrations instead of real concentrations as measured by CCN chambers (Roberts and Nenes, 2005); however, for simplicity, we refer to these

15 potential CCN as CCN hereafter.

This last analysis was not restricted to the months when the volcanic activity was detected, and all 193 NPF event days identified in 2015 were included in the analysis (167 non-plume days and 26 plume days). As reported earlier by Foucart et al. (2018), the growth of particles > 80 – 100 nm was observed as a common feature of a large majority of the investigated days besides NPF, regardless the occurrence of plume conditions. In addition, high background concentrations were frequently seen

20 above ~ 50 nm, most likely caused by the transport of pre-existing particles to the station. The influence of these phenomena on the variations of N_{80} and N_{100} was obvious, and often hindered the identification of a concurrent impact of NPF on the particle concentration increase at these sizes. In contrast, the background concentration was often significantly lower at 50 nm, which made it easier to unambiguously assess the growth of the newly formed particles up to 50 nm. Further evaluation of the contribution of NPF to the formation of CCN was thus finally performed using this single activation diameter, assuming N_{50}

25 was a good proxy for the concentration of particles likely to act CCN, or to become CCN after experiencing further growth. The increase of N_{50} observed during the events was attributed (at least partly) to NPF on 70 days, 15 of them being plume days, among which 8 strong plume days, and the remaining 55 being non-plume days. On the other 123 event days included in the analysis, the contribution of NPF to the increase of N_{50} was more uncertain, but could not be excluded. Resulting frequencies of NPF contributing to the increase of > 50 nm CCN were thus 33% for non-plume days and 58% for plume days

30 (including strong plume days) and 66.7% for strong plume days alone (Fig. 9.a). The increase of N_{50} observed during NPF was in addition quantified: N_{50-MAX}, the maximum of N_{50} observed during the event was compared to N_{50-REF}, calculated as the two-hour average of N_{50} between 05:00 and 07:00 LT, prior to nucleation hours. Note that for a given NPF event, the identification of N_{50-MAX} was limited to the time period 07:00 - 19:00 LT, because of the fast change of air masses and / or

wind direction which is often observed at Maïdo after 19:00 LT (see Fig. S3 in the Supplementary). The absolute increase of N_{50} was further calculated as the difference between N_{50-MAX} and N_{50-REF}, and the median CCN productions observed in the different conditions are reported on Fig. 9.b. The median of the N_{50} absolute increase observed on non-event days was around 420 cm^{-3}, and was significantly enhanced on event days, being around 1600 cm^{-3} on non-plume days and 3720 cm^{-3} in plume

5   conditions~~, reaching up to 3170 cm^{-3} when focussing on strong plume days only~~. The more pronounced concentration increase observed on event days, and in specific in plume conditions, was explained by the multiplication of the sources of such particles on those specific days. Indeed, on non-event days, the variations of N_{50} observed at Maïdo were probably caused exclusively by the transport of pre-existing large particles originating from the nearest urban areas. This process was itself tightly connected to the dynamics of the boundary layer and associated wind pattern, resulting in maximum concentrations around 13:00 LT (i.e.

10   09:00 UTC), as evidenced on Fig. 9.d. On event days, the diurnal variation of N_{50} was strengthened due to the concurrent formation of secondary aerosols, i.e. including the formation and growth of new particles as well as the growth of pre-existing larger particles mentioned earlier (Fig. 9.d). Additional contribution of large particles formed *via* heterogeneous processes close to the vent of the volcano (and denoted as volcanic primary particles in the present work) was finally highly probable in plume conditions, as discussed in Sect. 3.2.1 and 3.3.1. This last hypothesis was further supported by the increased level of

15   N_{50} observed during the night on plume days~~, and especially on strong plume days,~~ compared to other days (Fig. 9.d).

In a similar way as done previously by Rose et al. (2017), we made an attempt to decouple the contributions of the abovementioned CCN sources on event days. For that purpose, the transport of pre-existing large particles from the boundary layer was first assumed to have similar magnitude on event and non-event days, regardless the occurrence of plume conditions. We also made the assumption that the contribution of volcanic primary particles did not vary significantly along the day in

20   plume conditions, and was thus systematically removed when calculating the difference between N_{50-MAX} and N_{50-REF}. Following these hypotheses, the contribution of secondary aerosols to the observed CCN population was estimated from the difference between the median of the N_{50} absolute increase observed on event days (i.e. resulting from transport of particles from the boundary layer and secondary aerosol formation) and that of non-event days (resulting from transport only). Resulting concentrations attributed to secondary aerosols were ~ 1180 cm^{-3} and ~ 3300 cm^{-3} ~~and ~ 2750 cm^{-3}~~ for non-plume and plume

25   ~~and strong plume~~ event days, respectively, and dominated the increase of N_{50} observed on event days. From these average concentrations we could also infer the formation of secondary aerosols prone to act as CCN in plume conditions, with ~ 2120 cm^{-3} additional particles detected on regular plume days ~~and ~ 1570 cm^{-3} on strong plume days~~ compared to non-plume days. This stronger increase of the CCN concentration was most likely explained by the larger amount of condensable vapours available in plume conditions, including in specific sulfuric acid, as evidenced on Fig. 9.c. Indeed, the most significant N_{50}

30   increases coincided with high [H_2SO_4], suggesting that the growth of ~~the newly formed~~ more particles to CCN relevant sizes was favoured during NPF events occurring in the presence of large amount of H_2SO_4 caused by the eruptions. The increase of N_{50} due to secondary aerosol formation in the presence of the plume was also consistent and of the same order of magnitude as the increase of the particle concentration reported in similar conditions for the Aitken and accumulation modes in the previous section.

4. Summary and conclusions

We investigated the occurrence of NPF in volcanic plume conditions at the Maïdo observatory based on measurements conducted between January 1st and December 31st 2015. During this time period, 4 effusive eruptions of the Piton de la Fournaise, located ~ 39 km away from the station, were observed, and we were able to detect volcanic plume conditions at

5   Maïdo during 3 of the 4 eruptions. In total, 29 "plume days" were identified according to SO_2 mixing ratios measured during morning hours (06:00 – 11:00 LT, i.e. including usual nucleation hours), among which 14 days classified as "strong plume days", and were compared with 250 "non-plume days". This dataset is, to our knowledge, the largest ever reported for the investigation of NPF in volcanic plume conditions, and allowed for the first time a statistical approach to characterize the process and also assess its relevance with respect to non-plume conditions.

10 Focussing on the months during which the volcanic plume was detected at Maïdo (May, August, September and October), NPF was observed on 90% of the plume days vs 71% of the non-plume days. On plume days, when higher amounts of precursors (such as SO_2) were available prior to sunrise due to the occurrence of plume conditions, NPF seemed to be mainly limited by photochemistry, and was triggered early after sunrise. The process was in contrast observed later on non-plume days, most likely due to the lack of precursors before their transport from lower altitude after sunrise, as a result of convection.

15 With the exception of September, particle formation rates, both J_{12} and J_2, were on average significantly increased on plume days. In contrast, despite high values of GR_{12-19} reported on strong plume days, the overall effect of plume conditions on particle growth between 12 and 19 nm appeared to be limited, most likely because the number concentration of particles to grow was significantly raised in plume conditions, as reflected also by the larger CS observed on plume days. In contrast, with the exception of September, particle formation rates, both J_{12} and J_2, were on average significantly increased on plume days.

20 Signature of the volcanic plume on the aerosol spectra up to 600 nm was further investigated based on the analysis and fitting of the particle size distributions recorded in the different conditions. The spectra measured prior to nucleation hours (07:00 LT) gave a unique opportunity to compare the main features of the particle number size distributions recorded in plume and non-plume conditions in absence of freshly nucleated particles. Main differences were observed for the two accumulation modes (modal diameter ~ 100 and 190 nm, respectively), which were more densely populated in plume conditions compared

25 to non-plume days, most likely because of the contribution of particles formed *via* heterogeneous processes at the vent of the volcano during eruptive periods, and assimilated to primary volcanic particles in the present work. The particle size distribution only experienced limited changes on non-event days, but significant variations of the particle concentration were in contrast observed for the nucleation and Aitken modes on NPF event days between 08:00 and ~11:00 LT, especially in plume conditions. An average size distribution of the particles of volcanic origin was further inferred from the measurements

30 performed on event days in and off-plume conditions. The contribution of secondary particles to the total concentration was around 93%, and clearly dominated that of primary particles for all but the first accumulation mode concentration, for which primary particles contributed significantly (40%).

Specific attention was further paid to the concentration of particles > 50 nm (N_{50}), assuming they could be used as a proxy for potential CCN population. The variations of N_{50} were limited on non-event days, and attributed mainly to the vertical transport of pre-existing particles from the boundary layer, evaluated to ~ 420 cm^{-3}. The contribution of secondary particles to the increase of N_{50} was more frequent in plume than off-plume conditions, and the magnitude of the increase due to secondary

5   aerosol formation was ~ 3300 cm^{-3} compared to ~ 1180 cm^{-3} on non-plume days.

In order to investigate deeper the influence of volcanic plume conditions on the occurrence of NPF and related effects on particle concentration, we first investigated the variations of several atmospheric parameters (temperature, relative humidity and global radiation). Similar patterns were observed in and off-plume conditions, without any specificity for the events observed on plume days. Attention was then paid to the variations of the condensation sink (CS) and [H_2SO_4], previously

10 reported to play a key role in the process. In order to avoid any interference with the CS increase caused by the newly formed particles themselves, we focussed on the CS slightly prior to nucleation hours. The comparison of non-plume NPF event and non-event days did not highlight any clear tendency over the months of interest for this study. In contrast, the median CS obtained on plume days were on average higher than those observed on non-plume days. Increased SO_2 mixing ratios measured concurrently in plume conditions most likely compensated for the strengthened loss rate of the vapours and let NPF happen in

15 the form of stronger events (with respect to J_{12} and J_2) compared to non-plume days, suggesting at the same time a key role of H_2SO_4 in the process, consistent with recent observations in the plumes of Etna and Stromboli (Sahyoun et al., 2019). In order to test this last hypothesis, we derived [H_2SO_4] from SO_2 mixing ratios using a proxy available in the literature (Mikkonen et al., 2011). Despite a moderate strength, the correlation between J_2 and [H_2SO_4] was found to be significant. In addition, we also evaluated the contribution of binary nucleation of $H_2SO_4 – H_2O$ to the observed events using the recent parameterization

20 by Määttänen et al. (2018). Within the uncertainties associated to our calculations, we showed that in plume conditions, predicted J_2 from calculated H_2SO_4 concentration were fair approximations of J_2 derived from the measured J_{12}, indicating that H_2SO_4 was the main nucleating species in the plume. This result also highlighted the possibility to get relatively good estimates of J_2 in absence of direct measurement of [H_2SO_4] and sub-3 nm particles concentration, but only from the knowledge of SO_2 mixing ratios. The use of the parameterization finally gave insights into the pathways responsible for the

25 formation of 2-nm cluster in plume conditions, and highlighted in specific the dominant role of ion-induced nucleation for [H_2SO_4] below ~ 8×10^8 cm^{-3}, while neutral pathways were in contrast the most efficient above this threshold.

All together, our observations show that, based on one year of data, volcanic plume conditions favour the formation of particles that frequently grow to CCN sizes within the first 40 km of the volcano's vent. The quantification of the contribution of primary vs secondary aerosol formation within an active volcanic eruption plume on a statistical basis contributes to better

30 understanding of this natural process, which might have contributed significantly to NPF and CCN formation in the pristine preindustrial era. Nonetheless, our study should be complemented in the future with a direct analysis of the precursor vapours involved in the process, as our approach to assess the role of H_2SO_4 was based on calculations and we cannot exclude the contribution of other compounds, such as for instance halogens, and in particular iodine compounds, which were previously identified in volcanic plumes (Aiuppa et al., 2009) and also reported to contribute to NPF in coastal zones (Sipilä et al., 2016).

5. Data availability

DMPS data are accessible from the EBAS website (http://ebas.nilu.no/). AIS and SO_2 data can be provided upon request.
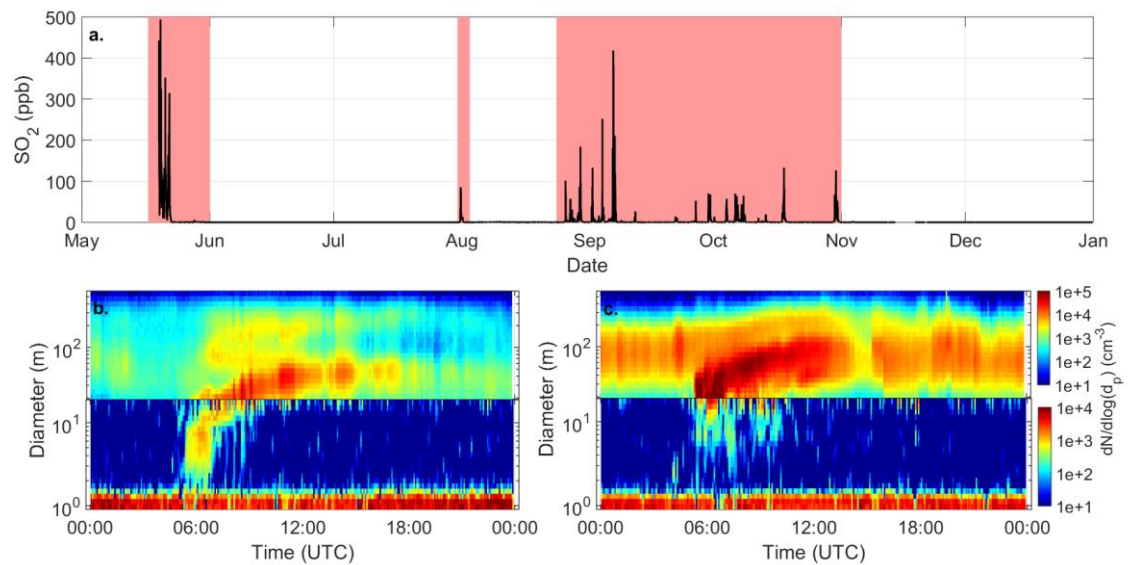

Figure 1 a. Timeseries of the SO_2 mixing ratio measured between May and December 2015 at Maïdo. The shaded areas highlight the three eruptive periods of the Piton de la Fournaise observed during this period. b. Negative ion (lower part) and particle (upper part) number size distributions showing an NPF event occurring on a regular plume day, on May 29th. c. Same as b. for the event detected on May 21st, in strong plume conditions. For b. and c., ion data was derived from AIS measurements, while particle concentrations were measured with the DMPS. Note the different colour scales for ion and particle measurements.
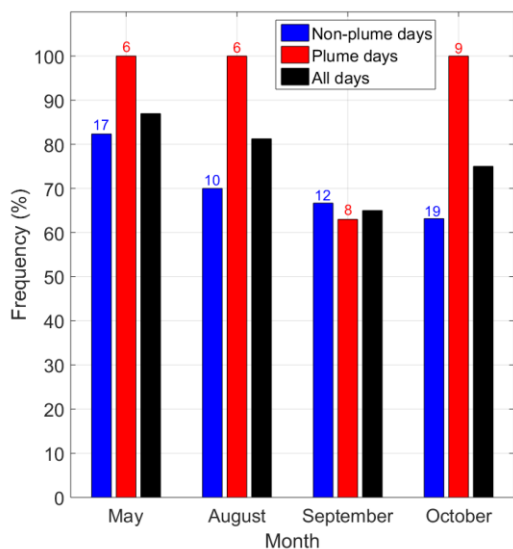
Figure 2 Frequency of occurrence of NPF at Maïdo. Statistics are shown separately for plume and non-plume days, and total frequencies are also reported. Numbers on the plot indicate, for plume and non-plume conditions, the total number of days included in the statistics.

5

10

15
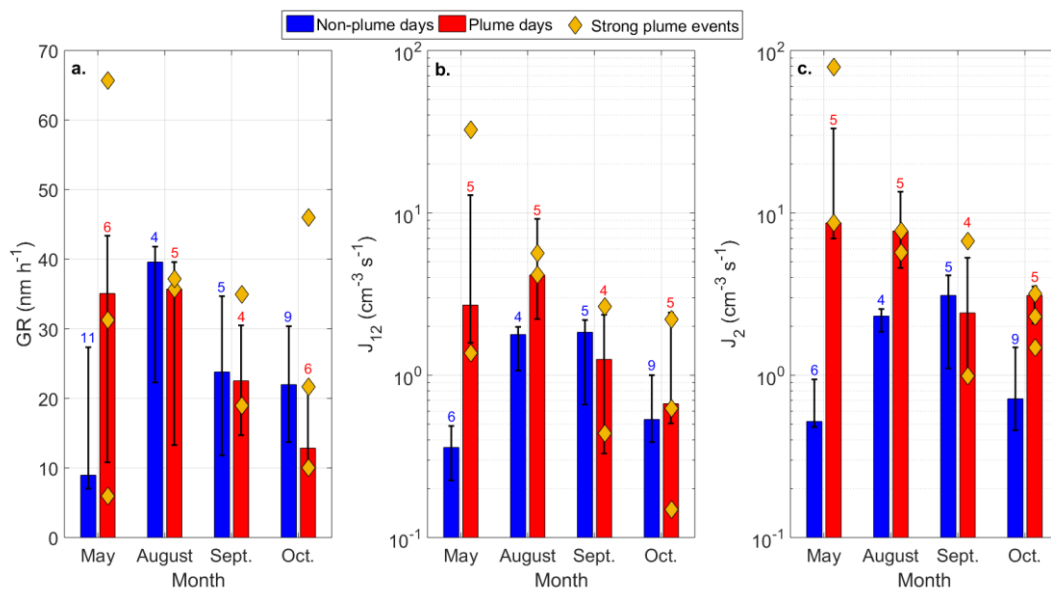
**Figure 3** Monthly medians and percentiles of the NPF event characteristics observed on plume and non-plume days at Maïdo. a. Particle growth rate between 12 and 19 nm (GR_{12-19}). Formation rate of b. 12 (J_{12}) and c. 2 nm (J_2) particles. The bars represent the median of the
20   data, and the lower and upper edges of the error bars indicate 25th and 75th percentiles, respectively. Data collected on strong plume days are included in the statistics reported for plume days and are also highlighted separately. Numbers on each plot indicate, for plume and non-plume conditions, the total number of NPF events included in the statistics.
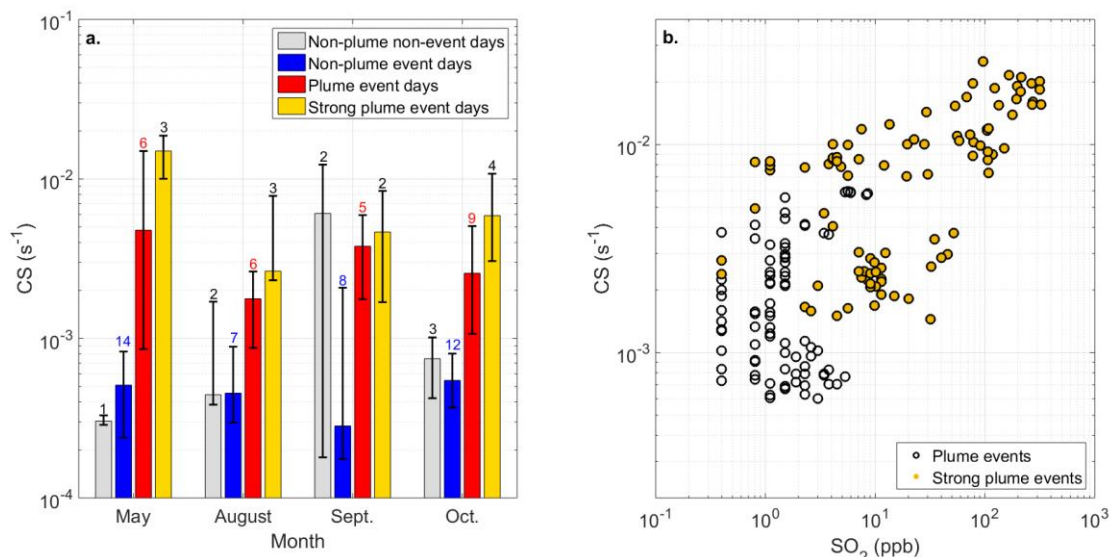
Figure 4 a. Monthly medians and percentiles of the CS measured prior to NPF hours (i.e. 05:00-07:00 LT). Note that strong plume days are included in the statistics reported for plume days and are also highlighted separately. See Fig. 3 for an explanation of symbols. Numbers on the plot indicate, for plume and non-plume conditions, event and non-event days, the total number of days included in the statistics. b. Link between the CS measured prior to NPF hours and SO_2 mixing ratios on plume days. Strong plume days are highlighted with specific markers.
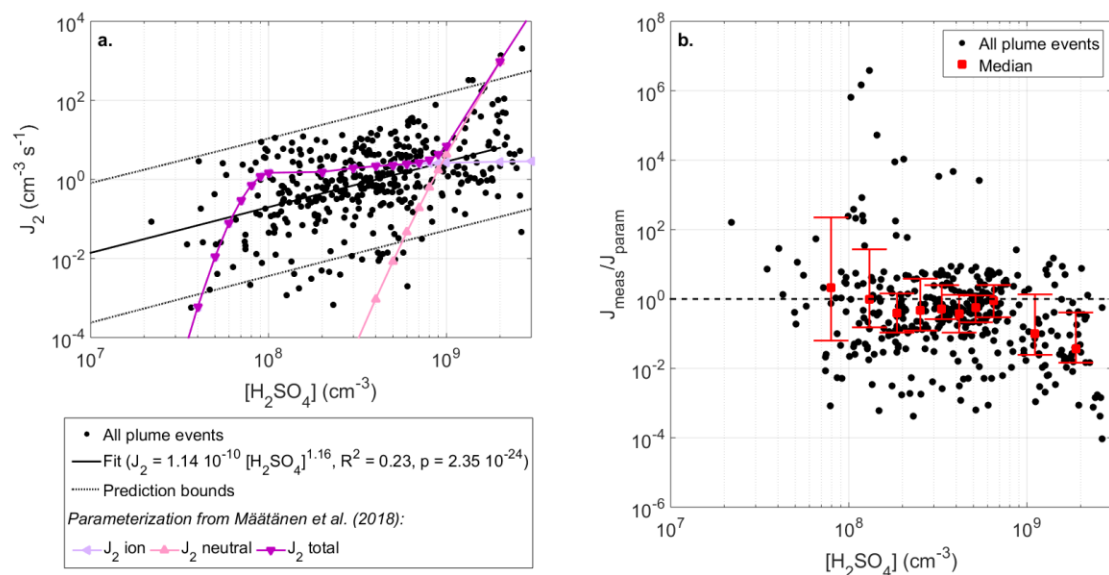
Figure 5 a. Correlation between the formation rate of 2 nm particles (J_2) and [H_2SO_4] on plume days. A power fit was performed on all available datapoints, as well as on those collected on strong plume days separately. The formation rates calculated from the parametrization by Määtänen et al. (2018), which describes the binary nucleation of H_2SO_4 – H_2O, are also shown, separately for charged (J_2 ion) and neutral (J_2 neutral) 2 nm clusters. The total formation rate (J_2 total) was additionally calculated as the sum of J_2 ion and J_2 neutral. b. Ratio between the 2 nm particle formation rates derived from DMPS measurements (J_{meas}) and the total formation rates derived from the parameterization (J_{param}) as a function of [H_2SO_4]. Data was also binned with respect to [H_2SO_4] (10 bins with equal number of points), and the medians

(squares) as well as the 25th/75th percentiles (error bars) of the ratio in each bin are presented. ~~Strong plume days are highlighted with specific markers.~~
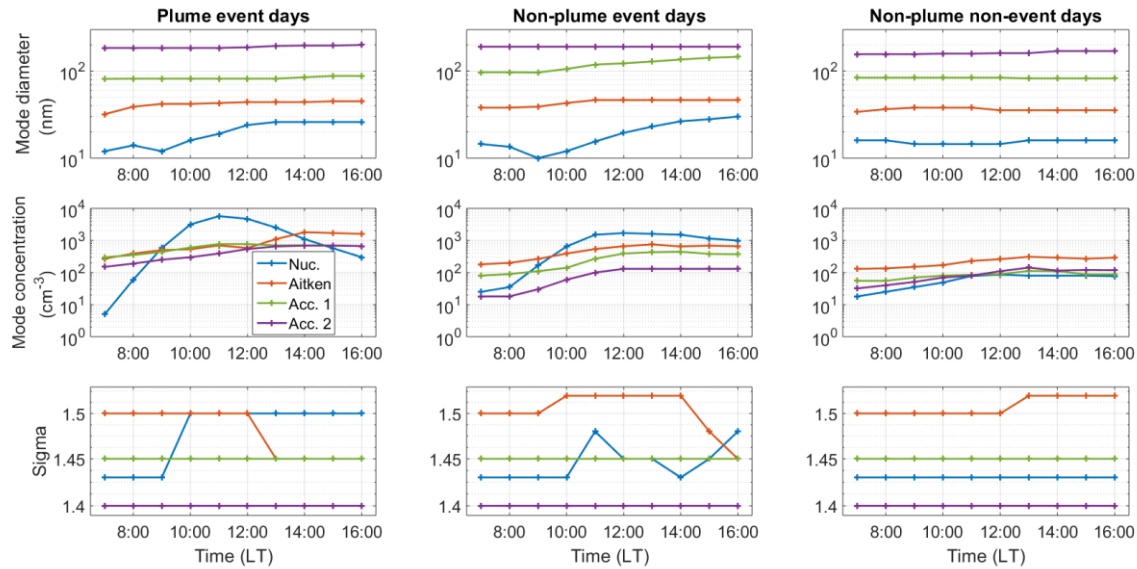
5
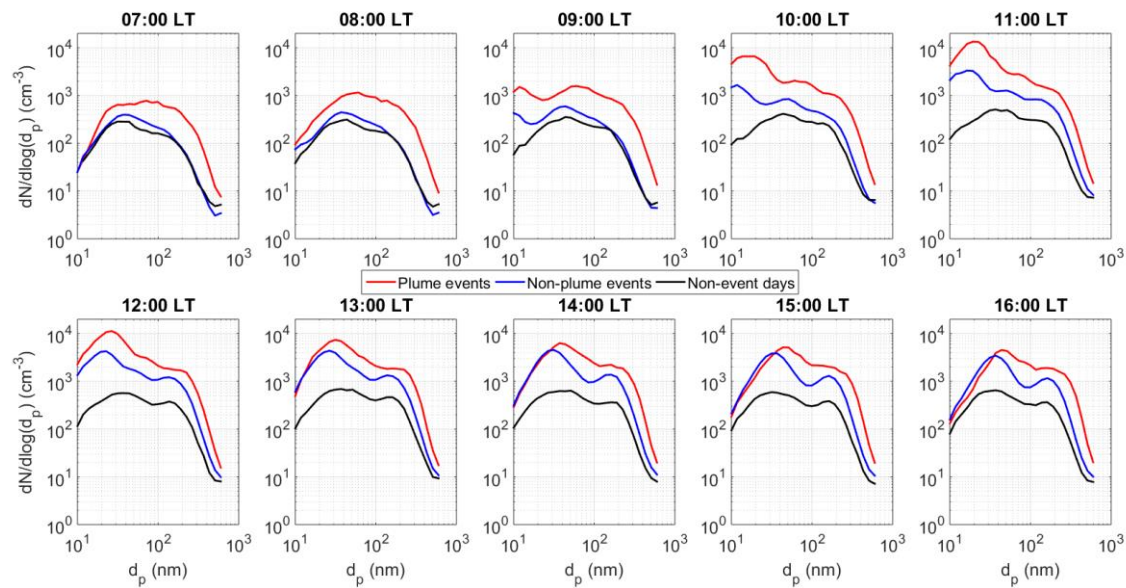
Figure 6 Hourly medians of the particle size distribution derived from DMPS measurements conducted in the different conditions (non-plume NPF event and non-event days, plume ~~and strong plume~~ NPF event days) between 07:00 and 16:00 LT. ~~Note that strong plume days are included in the statistics calculated for plume days, and are also highlighted separately.~~

10

15

Figure 7 Variations of the parameters of the Gaussians used to fit the hourly median DMPS size distributions shown on Fig. 6. ~~Note that strong plume days are included in the analysis conducted for plume days, but were not fitted separately.~~ All the displayed values are also reported in Table A1 of the Appendix.

5
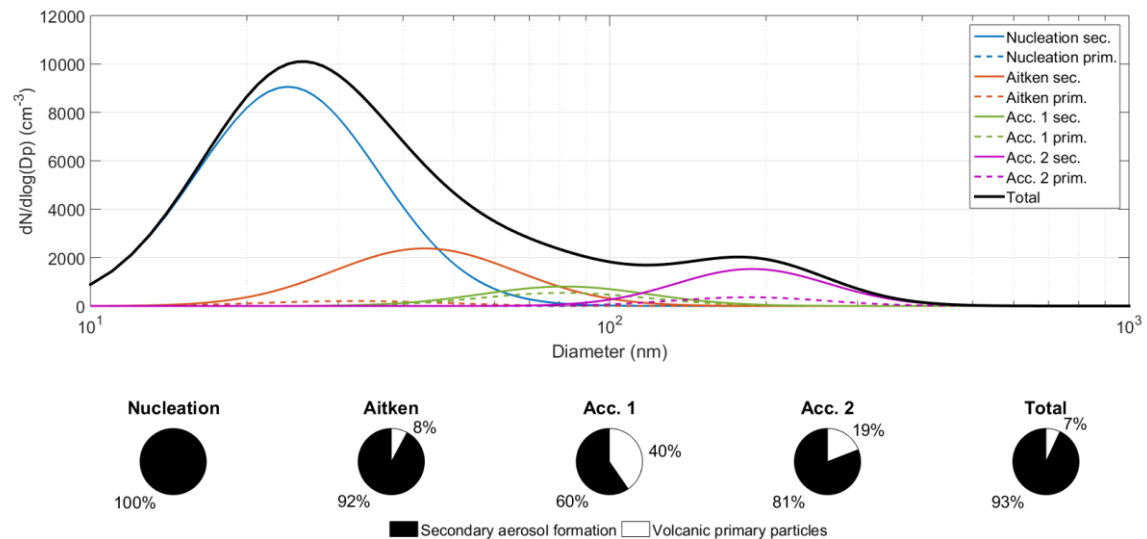
Figure 8 Size distribution of the particles of volcanic origin reconstructed using the spectra measured on plume and non-plume event days. The contributions of primary (i.e. formed/transformed *via* heterogeneous processes in the very close proximity of the vent) and secondary aerosols are shown separately for each mode on the spectrum and are further highlighted on the pie charts. The contribution of primary aerosols was evaluated based on the spectra measured at 07:00 LT in and off-plume conditions, while the contribution of secondary aerosols was deduced from the maximum concentrations measured for each mode in and off-plume conditions, between 11:00 and 14:00 LT.

10
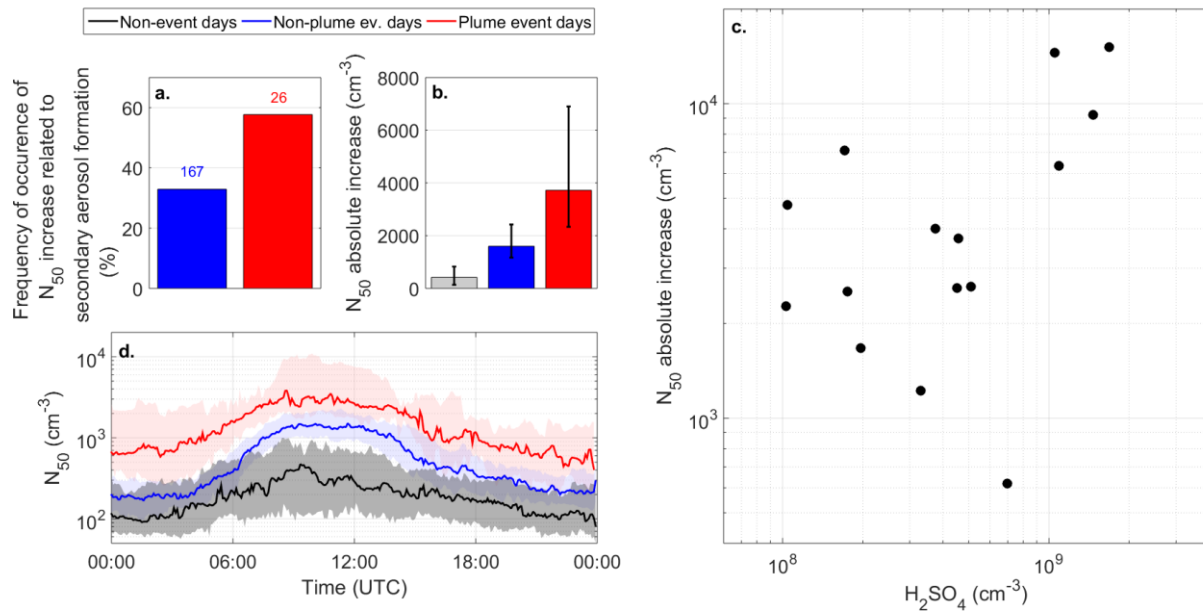
Figure 9 Increase of potential > 50 nm CCN particle concentration (N_{50}) during NPF in and off-plume conditions. a. Frequency of occurrence and b. magnitude of the absolute increase. ~~Note that strong plume days are included in the statistics reported for plume days and are also highlighted separately.~~ See Fig. 3 for an explanation of symbols. In a., numbers on the plot indicate, for non-plume and plume ~~and strong plume~~ conditions, the total number of NPF events included in the statistics. c. Link between the increase of N_{50} and [H_2SO_4] on plume days. ~~Strong plume days are highlighted with specific markers.~~ d. Median diurnal variation of N_{50} in the different conditions, including non-plume non-event days. Lower and upper limits of the shaded areas indicate the 25th and 75th percentiles of the data, respectively.

Appendix A

Table A1 Parameters of the Gaussians used to fit the hourly median DMPS size distributions shown on Fig. 6.

Type of days	Time (LT)	Nucleation mode			Aitken mode			1st accumulation mode			2nd accumulation mode		
		N (cm^{-3})	Sigma	d$_p$ (nm)	N (cm^{-3})	Sigma	d$_p$ (nm)	N (cm^{-3})	Sigma	d$_p$ (nm)	N (cm^{-3})	Sigma	d$_p$ (nm)
Plume event days	07:00	5	1.43	12.0	270	1.50	32.0	300	1.45	81.5	150	1.40	185.0
	08:00	60	1.43	14.0	390	1.50	39.0	350	1.45	82.0	190	1.40	185.0
	09:00	580	1.43	12.0	500	1.50	42.0	440	1.45	82.0	250	1.40	185.0
	10:00	3150	1.50	16.0	530	1.50	42.0	600	1.45	82.0	300	1.40	185.0
	11:00	5700	1.50	19.0	700	1.50	43.0	770	1.45	82.0	390	1.40	185.0
	12:00	4700	1.50	24.0	580	1.50	44.0	770	1.45	82.0	540	1.40	188.0
	13:00	2500	1.50	26.0	1100	1.45	44.0	700	1.45	82.0	650	1.40	195.0
	14:00	1100	1.50	26.0	1800	1.45	44.0	700	1.45	85.0	690	1.40	197.0
	15:00	570	1.50	26.0	1700	1.45	45.0	700	1.45	88.0	690	1.40	197.0
	16:00	300	1.50	26.0	1600	1.45	45.0	670	1.45	88.0	670	1.40	200.0
Non-plume event days	07:00	25	1.43	14.5	180	1.50	38.0	80	1.45	97.0	18	1.40	191.0
	08:00	35	1.43	13.5	200	1.50	38.0	90	1.45	97.0	18	1.40	191.0
	09:00	165	1.43	10.0	265	1.50	39.0	110	1.45	96.5	30	1.40	191.0
	10:00	650	1.43	12.0	390	1.52	43.0	140	1.45	106.0	60	1.40	191.0
	11:00	1500	1.48	15.5	540	1.52	46.5	270	1.45	119.0	100	1.40	191.0
	12:00	1700	1.45	19.5	660	1.52	46.5	390	1.45	123.0	130	1.40	191.0
	13:00	1600	1.45	23.0	750	1.52	46.5	430	1.45	129.0	130	1.40	191.0
	14:00	1500	1.43	26.5	650	1.52	46.5	445	1.45	136.0	130	1.40	191.0
	15:00	1150	1.45	28.0	690	1.48	46.5	380	1.45	142.5	130	1.40	191.0
	16:00	990	1.48	30.0	660	1.45	46.5	370	1.45	146.0	130	1.40	191.0
Non-plume non-event days	07:00	18	1.43	16.0	130	1.50	34.0	55	1.45	84.0	32	1.40	157.0
	08:00	25	1.43	16.0	135	1.50	36.5	55	1.45	84.0	40	1.40	157.0
	09:00	35	1.43	14.5	150	1.50	38.0	70	1.45	84.0	51	1.40	157.0
	10:00	49	1.43	14.5	170	1.50	38.0	80	1.45	84.0	70	1.40	159.0
	11:00	78	1.43	14.5	230	1.50	38.0	85	1.45	84.0	80	1.40	159.0
	12:00	86	1.43	14.5	260	1.50	35.5	89	1.45	84.0	110	1.40	161.0
	13:00	80	1.43	16.0	310	1.52	35.5	112	1.45	82.5	142	1.40	161.0
	14:00	80	1.43	16.0	290	1.52	35.5	110	1.45	82.5	115	1.40	170.0
	15:00	80	1.43	16.0	270	1.52	35.5	88	1.45	82.5	120	1.40	170.0
	16:00	77	1.43	16.0	290	1.52	35.5	88	1.45	82.5	118	1.40	170.0

Author contribution

K.S. and P.T. organized the measurements, J.-M.M. conducted the measurements, D.P. contributed to the design of the instrumental setup, C.R., B.F., K.S. and A.C. analysed the data, C.R. and K.S. wrote the manuscript, all authors commented on the manuscript.

5

Acknowledgements

Competing interest

No competing interest.

15   **References**

Aiuppa, A., Baker, D. R., and Webster, J. D.: Halogens in volcanic systems, Chemical Geology, 263, 1 – 18, doi:10.1016/j.chemgeo.2008.10.005, 2009.

Albrecht, B. A.: Aerosols, cloud microphysics, and fractional cloudiness, Science, 245(4923), 1227–1230, 1989.

Allen, A. G., Oppenheimer, C., Ferm, M., Baxter, P. J., Horrocks, L. A., Galle, B., McGonigle, A. J. S. and Duffell, H. J.:
20   Primary sulphate aerosol and associated emissions from Masaya Volcano, Nicaragua, J. Geophys. Res., 107(D23), doi:10.1029/2002JD002120, 2002.

Andres, R. J., and Kasgnoc, A. D.: A time-averaged inventory of subaerial volcanic sulfur emissions, J. Geophys. Res., 103(D19), 25251 - 25261, 1998.

Asmi, E., Freney, E., Hervo, M., Picard, D., Rose, C., Colomb, A., and Sellegri, K.: Aerosol cloud activation in summer and
25   winter at puy-de-Dôme high altitude site in France, Atmos. Chem. Phys., 12, 11589-11607, https://doi.org/10.5194/acp-12-11589-2012, 2012.

Baray, J.-L., Courcoux, Y., Keckhut, P., Portafaix, T., Tulet, P., Cammas, J.-P., Hauchecorne, A., Godin-Beekmann, S., De Mazière, M., Hermans, C. and others: Maïdo observatory: a new high-altitude station facility at Reunion Island (21° S, 55° E) for long-term atmospheric remote sensing and in situ measurements, Atmospheric Meas. Tech., 6(10), 2865–2877, 2013.

30   Berresheim, H., Adam, M., Monahan, C., O'Dowd, C., Plane, J. M. C., Bohn, B., and Rohrer, F.: Missing SO_2 oxidant in the coastal atmosphere? – observations from high-resolution measurements of OH and atmospheric sulfur compounds, Atmos. Chem. Phys., 14, 12209-12223, https://doi.org/10.5194/acp-14-12209-2014, 2014.

Birmili, W., Berresheim, H., Plass-Dülmer, C., Elste, T., Gilge, S., Wiedensohler, A., and Uhrner, U.: The Hohenpeissenberg aerosol formation experiment (HAFEX): a long-term study including size-resolved aerosol, H2SO4, OH, and monoterpenes measurements, Atmos. Chem. Phys., 3, 361-376, https://doi.org/10.5194/acp-3-361-2003, 2003.

Boulon, J., Sellegri, K., Venzac, H., Picard, D., Weingartner, E., Wehrle, G., Collaud Coen, M., Bütikofer, R., Flückiger, E., Baltensperger, U., and Laj, P.: New particle formation and ultrafine charged aerosol climatology at a high altitude site in the Alps (Jungfraujoch, 3580 m a.s.l., Switzerland), Atmos. Chem. Phys., 10, 9333-9349, https://doi.org/10.5194/acp-10-9333-2010, 2010.

Boulon, J., Sellegri, K., Hervo, M., Picard, D., Pichon, J.-M., Fréville, P., and Laj, P.: Investigation of nucleation events vertical extent: a long term study at two different altitude sites, Atmos. Chem. Phys., 11, 5625–5639, doi:10.5194/acp-11-56252011, 2011.

Boulon, J., Sellegri, K., Hervo, M., and Laj, P.: Observations of nucleation of new particles in a volcanic plume, Proc. Natl. Acad. Sci. U.S.A., 108, 12223 – 12226, 2011.

Carslaw, K. S., Lee, L. A., Reddington, C. L., Pringle, K. J., Rap, A., Forster, P. M., Mann, G. W., Spracklen, D. V., Woodhouse, M. T., Regayre, L. A., and Pierce, J. R., Large contribution of natural aerosols to uncertainty in indirect forcing, Nature, 503, 67 – 71, 2013.

Dada, L., Paasonen, P., Nieminen, T., Buenrostro Mazon, S., Kontkanen, J., Peräkylä, O., Lehtipalo, K., Hussein, T., Petäjä, T., Kerminen, V.-M., Bäck, J., and Kulmala, M.: Long-term analysis of clear-sky new particle formation events and nonevents in Hyytiälä, Atmos. Chem. Phys., 17, 6227-6241, https://doi.org/10.5194/acp-17-6227-2017, 2017.

Deshler, T., Hofmann, D. J., Johnson, B. J., and Rozier, W. R.: Balloonborne measurements of the Pinatubo aerosol size distribution and volatility at Laramie, Wyoming during the summer of 1991, Geophys. Res. Let., 19(2), 199-202, 1992.

Di Muro, A. , Staudacher, T. , Ferrazzini, V. , Métrich, N. , Besson, P. , Garofalo, C. and Villemant, B. (2015). Shallow Magma Storage at Piton de la Fournaise Volcano After 2007 Summit Caldera Collapse Tracked in Pele's Hairs. In Hawaiian Volcanoes, edited by Carey, R., Cayol, V., Poland, M. and Weis, D., doi:10.1002/9781118872079.ch9, 2015.

Duflot, V., Dils, B., Baray, J. L., De Mazière, M., Attié, J. L., Vanhaelewyn, G., Senten, C., Vigouroux, C., Clain, G., and Delmas, R.: Analysis of the origin of the distribution of CO in the subtropical southern Indian Ocean in 2007, J. Geophys. Res., 115, D22106, doi:10.1029/2010JD013994, 2010.

Duplissy, J., Merikanto, J., Franchin, A., Tsagkogeorgas, G., Kangasluoma, J., Wimmer, D., Vuollekoski, H., Schobesberger, S., Lehtipalo, K., Flagan, R. C., Brus, D., Donahue, N. M., Vehkamäki, H., Almeida, J., Amorim, A., Barmet, P., Bianchi, F., Breitenlechner, M., Dunne, E. M., Guida, R., Henschel, H., Junninen, H., Kirkby, J., Kürten, A., Kupc, A., Määttänen, A., Makhmutov, V., Mathot, S., Nieminen, T., Onnela, A., Praplan, A. P., Riccobono, F., Rondo, L., Steiner, G., Tome, A., Walther, H., Baltensperger, U., Carslaw, K. S., Dommen, J., Hansel, A., Petäjä, T., Sipilä, M., Stratmann, F., Vrtala, A., Wagwww.atmos-chem-phys.net/17/14171/2017/ Atmos. Chem. Phys., 17, 14171–14180, 2017 14178 J. Lengyel et al.: Electron-induced chemistry in microhydrated sulfuric acid clusters ner, P. E., Worsnop, D. R., Curtius, J., and Kulmala, M.: Effect of ions on sulfuric acid-water binary particle formation: 2. Experimental data and comparison with QC-normalized classical nucleation theory, J. Geophys. Res.-Atmos., 121, 1752–1775, https://doi.org/10.1002/2015JD023539, 2016.

Foucart, B., Sellegri, K., Tulet, P., Rose, C., Metzger, J.-M., and Picard, D.: High occurrence of new particle formation events at the Maïdo high-altitude observatory (2150 m), Réunion (Indian Ocean), Atmos. Chem. Phys., 18, 9243-9261, https://doi.org/10.5194/acp-18-9243-2018, 2018.

Gordon, H., Sengupta, K., Rap, A., Duplissy, J., Frege, C., Williamson, C., Heinritzi, M., Simon, M., Yan, C., Almeida, J., Tröstl, J., Nieminen, T., Ortega, I. K., Wagner, R., Dunne, E. M., Adamov, A., Amorim, A., Bernhammer, A.-K., Bianchi, F., Breitenlechner, M., Brilke, S., Chen, X., Craven, J. S., Dias, A., Ehrhart, S., Fischer, L., Flagan, R. C., Franchin, A., Fuchs, C., Guida, R., Hakala, J., Hoyle, C. R., Jokinen, T., Junninen, H., Kangasluoma, J., Kim, J., Kirkby, J., Krapf, M., Kürten, A.,
5 Laaksonen, A., Lehtipalo, K., Makhmutov, V., Mathot, S., Molteni, U., Monks, V, Onnela, A., Peräkylä, O., Piel, F., Petäjä, T., Praplan, A. P., Pringle, K. J., Richards, N. A. D., Rissanen, M. P., Rondo, L., Sarnela, N., Schobesberger, S., Scott, C. E., Seinfield, J. H., Sharma, S., Sipilä, M., Steiner, G., Stozhkov, Y., Stratmann, F., Tomé, A., Virtanen, A., Vogel, A. L., Wagner, A. C., Wagner, P. E., Weingartner, E., Wimmer, D., Winkler, P. M., Ye, P., Zhang, X., Hansel, A., Dommen, J., Donahue, N. M., Worsnop, D. R., Baltensperger, U., Kulmala, M., Curtius, J., and Carslaw, K. S.: Reduced anthropogenic aerosol radiative
10 forcing caused by biogenic new particle formation, Proc. Natl. Acad. Sci. U.S.A., 113, 12053–12058, 2016.

Gordon, H., Kirkby, J., Baltensperger, U., Bianchi, F., Breitenlechner, M., Curtius, J., Dias, A., Dommen, J., Donahue, N., Dunne, E., Duplissy, J., Ehrhart, S., Flagan, R., Ferge, C., Fuchs, C., Hansel, A., Hoyle, C., Kulmala, M., Kürten, A., Lehtipalo, K., Makhmutov, V., Molteni, U., Rissanen, M., Stozhkov, Y., Tröstl, J., Tsagkogeorgas, G., Wagner, R., Williamson, C., Wimmer, D., Winkler, P., Yan, C., and Carslaw, K.: Causes and importance of new particle formation in the present-day and
15 preindustrial atmospheres, J. Geophys. Res.-Atmos., 122, 8739–8760, https://doi.org/10.1002/2017JD026844, 2017.

Hammer, E., Bukowiecki, N., Gysel, M., Jurányi, Z., Hoyle, C. R., Vogt, R., Baltensperger, U., and Weingartner, E.: Investigation of the effective peak supersaturation for liquid-phase clouds at the high-alpine site Jungfraujoch, Switzerland (3580ma.s.l.), Atmos. Chem. Phys., 14, 1123–1139, doi:10.5194/acp-14-11232014, 2014.

Hervo, M., Quennehen, B., Kristiansen, N. I., Boulon, J., Stohl, A., Fréville, P., Pichon, J.-M., Picard, D., Labazuy, P., Gouhier,
20 M., Roger, J.-C., Colomb, A., Schwarzenboeck, A., and Sellegri, K.: Physical and optical properties of 2010 Eyjafjallajökull volcanic eruption aerosol: ground-based, Lidar and airborne measurements in France, Atmos. Chem. Phys., 12, 1721-1736, https://doi.org/10.5194/acp-12-1721-2012, 2012.

Hirsikko, A., Laakso, L., Horrak, U., Aalto, P. P., Kerminen, V. and Kulmala, M.: Annual and size dependent variation of growth rates and ion concentrations in boreal forest, Boreal Environ. Res., 10(5), 357, 2005.

25 Hirsikko, A., Vakkari, V., Tiitta, P., Manninen, H. E., Gagné, S., Laakso, H., Kulmala, M., Mirme, A., Mirme, S., Mabaso, D., Beukes, J. P. and Laakso, L.: Characterisation of sub-micron particle number concentrations and formation events in the western Bushveld Igneous Complex, South Africa, Atmos. Chem. Phys., 12(9), 3951–3967, doi:10.5194/acp12-3951-2012, 2012.

Jokinen, T., Sipilä, M., Junninen, H., Ehn, M., Lönn, G., Hakala, J., Petäjä, T., Mauldin III, R. L., Kulmala, M., and Worsnop,
30 D. R.: Atmospheric sulphuric acid and neutral cluster measurements using CI-APi-TOF, Atmos. Chem. Phys., 12, 4117-4125, https://doi.org/10.5194/acp-12-4117-2012, 2012.

Junninen, H., Ehn, M., Petäjä, T., Luosujärvi, L., Kotiaho, T., Kostiainen, R., Rohner, U., Gonin, M., Fuhrer, K., Kulmala, M., and Worsnop, D. R.: A high-resolution mass spectrometer to measure atmospheric ion composition, Atmos. Meas. Tech., 3, 1039-1053, https://doi.org/10.5194/amt-3-1039-2010, 2010.

35 Jurányi, Z., Gysel, M., Weingartner, E., Bukowiecki, N., Kammermann, L., and Baltensperger, U.: A 17 month climatology of the cloud condensation nuclei number concentration at the high alpine site Jungfraujoch, J. Geophys. Res., 116, D10204, doi:10.1029/2010JD015199, 2011.

Kerminen, V.-M., Paramonov, M., Anttila, T., Riipinen, I., Fountoukis, C., Korhonen, H., Asmi, E., Laakso, L., Lihavainen, H., Swietlicki, E., Svenningsson, B., Asmi, A., Pandis, S. N., Kulmala, M., and Petäjä, T.: Cloud condensation nuclei
40 production associated with atmospheric nucleation: a synthesis based on existing literature and new results, Atmos. Chem. Phys., 12, 12037– 12059, doi:10.5194/acp-12-12037-2012, 2012.

Kerminen, V.-M., Chen, X., Vakkari, V., Petäjä, T., Kulmala, M., and Bianchi, F.: Atmospheric new particle formation and growth: review of field observations, Environ. Res. Lett., 10, https://doi.org/10.1088/1748-9326/aadf3c, 2018.

Kuang, C., McMurry, P. H., McCormick, A. V. and Eisele, F. L.: Dependence of nucleation rates on sulfuric acid vapor concentration in diverse atmospheric locations, J. Geophys. Res. Atmospheres, 113(D10), https://doi.org/10.1029/2007JD009253, 2008.

Kulmala, M., Lehtinen, K. E. J. and Laaksonen, A.: Cluster activation theory as an explanation of the linear dependence between formation rate of 3nm particles and sulphuric acid concentration, Atmos Chem Phys, 6(3), 787–793, doi:10.5194/acp-6-787-2006, 2006.

Kulmala, M., Petäjä, T., Nieminen, T., Sipilä, M., Manninen, H. E., Lehtipalo, K., Dal Maso, M., Aalto, P. P., Junninen, H., and Paasonen, P.: Measurement of the nucleation of atmospheric aerosol particles, Nat. Protoc., 7, 1651–1667, doi:10.1038/nprot.2012.091, 2012.

Kulmala, M., Kontkanen, J., Junninen, H., Lehtipalo, K., Manninen, H. E., Nieminen, T., Petäjä, T., Sipilä, M., Schobesberger, S., Rantala, P., Franchin, A., Jokinen, T., Järvinen, E., Äijälä, M., Kangasluoma, J., Hakala, J., Aalto, P. P., Paasonen, P., Mikkilä, J., Vanhanen, J., Aalto, J., Hakola, H., Makkonen, U., Ruuskanen, T., Mauldin, R. L., Duplissy, J., Vehkamäki, H., Bäck, J., Kortelainen, A., Riipinen, I., Kurtén, T., Johnston, M. V., Smith, J. N., Ehn, M., Mentel, T. F., Lehtinen, K. E. J., Laaksonen, A., Kerminen, V.-M. and Worsnop, D. R.: Direct Observations of Atmospheric Aerosol Nucleation, Science, 339(6122), 943–946, doi:10.1126/science.1227385, 2013.

Lehtinen, K. E. J., Dal Maso, M., Kulmala, M. and Kerminen, V.-M.: Estimating nucleation rates from apparent particle formation rates and vice versa: Revised formulation of the Kerminen–Kulmala equation, J. Aerosol Sci., 38(9), 988–994, doi:10.1016/j.jaerosci.2007.06.009, 2007.

Määttänen, A., Merikanto, J., Henschel, H., Duplissy, J., Makkonen, R., Ortega, I. K., and Vehkamäki, H.: New parameterizations for neutral and ion-induced sulfuric acid – water particle formation in nucleation and kinetic regimes, J. Geophys. Res., 123, 1269 – 1296, https://doi.org/10.1002/2017JD027429, 2018.

Makkonen, R., Asmi, A., Kerminen, V.-M., Boy, M., Arneth, A., Hari, P., and Kulmala, M.: Air pollution control and decreasing new particle formation lead to strong climate warming, Atmos. Chem. Phys., 12, 1515–1524, doi:10.5194/acp-12-15152012, 2012.

Mallik, C., Ghosh, D., Ghosh, D., Sarkar, U., Lal, S., and Venkataramani, S.: Variability of SO2, CO, and light hydrocarbons over a megacity in Eastern India: effects of emissions and transport, Environ. Sci. Pollut. Res., 21(14), 8692-8706, https://doi.org/10.1007/s11356-014-2795-x, 2014.

Mather, T. A.: Volcanoes and the environment: Lessons for understanding Earth's past and future from studies of present-day volcanic emissions, Journal of Volcanology and Geothermal Research, 304, 160-179, 2015.

Mauldin III, R. L., Cantrell, C. A., Zondlo, M., Kosciuch, E., Eisele, F. L., Chen, G., Davis, D., Weber, R., Crawford, J., Blake, D., Bandy, A., and Thornton, D.: Highlights of OH, H2SO4, and methane sulfonic acid measurements made aboard the NASA P-3B during Transport and Chemical Evolution over the Pacific, J. Geophys. Res., 108(D20), 8796, doi:10.1029/2003JD003410, 2003.

Merikanto, J., Spracklen, D. V., Mann, G. W., Pickering, S. J., and Carslaw, K. S.: Impact of nucleation on global CCN, Atmos. Chem. Phys., 9, 8601–8616, doi:10.5194/acp-9-8601-2009, 2009.

Mikkonen, S., Romakkaniemi, S., Smith, J. N., Korhonen, H., Petäjä, T., Plass-Duelmer, C., Boy, M., McMurry, P. H., Lehtinen, K. E. J., Joutsensaari, J., Hamed, A., Mauldin III, R. L., Birmili, W., Spindler, G., Arnold, F., Kulmala, M., and Laaksonen, A.: A statistical proxy for sulphuric acid concentration, Atmos. Chem. Phys., 11, 11319–11334, doi:10.5194/acp-11-11319-2011, 2011.

5   Mirme, A., Tamm, E., Mordas, G., Vana, M., Uin, J., Mirme, S., Bernotas, T., Laakso, L., Hirsikko, A. and Kulmala, M.: A widerange multi-channel Air Ion Spectrometer, Boreal Environ. Res., 12(3), 247–264, 2007.

Myhre, G., Shindell, D., Bréon, F.-M., Collins, W., Fuglestvedt, J., Huang, J., Koch, D., Lamarque, J.-F., Lee, D., Mendoza, B., Nakajima, T., Robock, A., Stephens, G., Takemura, T., and Zhang, H.: Anthropogenic and Natural Radiative Forcing, Contribution of Working Group I to the Fifth Assessment Report of the Intergovernmental Panel on Climate Change, edited
10 by Stocker, T.F., Qin, D., Plattner, G.-K., Tignor, M., Allen, S.K., Boschung, J., Nauels, A., Xia, Y., Bex, V., and Midgley, P.M., Cambridge University Press, Cambridge, United Kingdom and New York, NY, USA, 2013.

Penner, J.E., Andreae, M., Annegarn, H., Barrie, L., Feichter, J., Hegg, D., Jayaraman, A., Leaitch, R., Murphy, D., Nganga, J., and Pitari, G.: Aerosols, their direct and indirect effects, Contribution of Working Group I to the Third Assessment Report of the Intergovernmental Panel on Climate Change, edited by B. Nyenzi, B., and Prospero, J., Cambridge University Press,
15 Cambridge, United Kingdom and New York, NY, USA, 2001.

Petäjä, T., Mauldin, III, R. L., Kosciuch, E., McGrath, J., Nieminen, T., Paasonen, P., Boy, M., Adamov, A., Kotiaho, T., and Kulmala, M.: Sulfuric acid and OH concentrations in a boreal forest site, Atmos. Chem. Phys., 9, 7435–7448, doi:10.5194/acp9-7435-2009, 2009.

Roberts, G. C. and Nenes, A.: A continuous-flow streamwise thermal-gradient CCN chamber for atmospheric measurements,
20 Aerosol Sci. Technol., 39, 206–221, 2005.

Robert, T., Dayma, G. and Oppenheimer, C.: Reaction rates control high-temperature chemistry of volcanic gases in air, Front. Earth Sci., doi:10.3389/feart.2019.00154, 2019.

Robock, A.: Volcanic eruptions and climate, Reviews of Geophysics, 38, 191 – 219, 2000.

Rose, C., Boulon, J., Hervo, M., Holmgren, H., Asmi, E., Ramonet, M., Laj, P., and Sellegri, K.: Long-term observations of
25 cluster ion concentration, sources and sinks in clear sky conditions at the high-altitude site of the Puy de Dôme, France, Atmos. Chem. Phys., 13, 11573-11594, https://doi.org/10.5194/acp-13-11573-2013, 2013.

Rose, C., Sellegri, K., Velarde, F., Moreno, I., Ramonet, M., Weinhold, K., Krejci, R., Andrade, M., Wiedensohler, A., and Laj, P.: Frequent nucleation events at the high-altitude station of Chacaltaya (5240ma.s.l.), Bolivia, Atmos. Environ., 102, 18–29, doi:10.1016/j.atmosenv.2014.11.015, 2015.
30
Rose, C., Sellegri, K., Moreno, I., Velarde, F., Ramonet, M., Weinhold, K., Krejci, R., Andrade, M., Wiedensohler, A., Ginot, P., and Laj, P.: CCN production by new particle formation in the free troposphere, Atmos. Chem. Phys., 17, 1529-1541, https://doi.org/10.5194/acp-17-1529-2017, 2017.

Rosenfeld, D., Sherwood, S., Wood, R. and Donner, L.: Climate Effects of Aerosol Cloud Interactions, Science, 343(6169),
35 379–380, doi:10.1126/science.1247490, 2014.

Sahyoun, M., Freney, E., Brito, J., Duplissy, J., Gouhier, M., Colomb, A., Dupuy, R., Bourianne, T., Nowak, J. B., Yan, C., Petäjä, T., Kulmala, M., Schwarzenboeck, A., Planche, C. and Sellegri, K.: Evidence of new particle formation within Etna and Stromboli volcanic plumes and its parameterization from airborne in-situ measurements, J. Geophys. Res.-Atmos, https://doi.org/10.1029/2018JD028882, 2019.

Schmidt, A., Carslaw, K. S., Mann, G. W., Rap, A., Pringle, K. J., Spracklen, D. V., Wilson, M., and Forster, P. M.: Importance of tropospheric volcanic aerosol for indirect radiative forcing of climate, Atmos. Chem. Phys., 12, 7321-7339, https://doi.org/10.5194/acp-12-7321-2012, 2012.

Seinfeld, J.H. and Pandis, S.N.: Atmospheric Chemistry and Physics: From Air Pollution to Climate Change, 2nd Edition, John Wiley & Sons, New York, 2006.

Sihto, S.-L., Kulmala, M., Kerminen, V.-M., Dal Maso, M., Petäjä, T., Riipinen, I., Korhonen, H., Arnold, F., Janson, R., Boy, M., Laaksonen, A. and Lehtinen, K. E. J.: Atmospheric sulphuric acid and aerosol formation: implications from atmospheric measurements for nucleation and early growth mechanisms, Atmos Chem Phys, 6(12), 4079–4091, doi:10.5194/acp-6-40792006, 2006.

Sipilä, M., Berndt, T., Petäjä, T., Brus, D., Vanhanen, J., Stratmann, F., Patokoski, J., Mauldin, R. L., Hyvärinen, A.-P., Lihavainen, H. and Kulmala, M.: The Role of Sulfuric Acid in Atmospheric Nucleation, Science, 327(5970), 1243–1246, doi:10.1126/science.1180315, 2010.

Sipilä, M., Sarnela, N., Jokinen, T., Henschel, H., Junninen, H., Kontkanen, J., Richters, S., Kangasluoma, J., Franchin, A., Peräkylä, O., Rissanen, M. P., Ehn, M., Vehkamäki, H., Kurten, T., Berndt, T., Petäjä, T., Worsnop, D., Ceburnis, D., Kerminen, V.-M., Kulmala, M., and O'Dowd, C.: Molecular-scale evidence of aerosol particle formation via sequential addition of HIO3, Nature, 537, 532-534, doi:10.1038/nature19314, 2016.

Tröstl, J., Herrmann, E., Frege, C., Bianchi, F., Molteni, U., Bukowiecki, N., Hoyle, C. R., Steinbacher, M., Weingartner, E., Dommen, J., Gysel, M., and Baltensperger, U.: Contribution of new particle formation to the total aerosol concentration at the high altitude site Jungfraujoch (3580ma.s.l., Switzerland), J. Geophys. Res.-Atmos., 121, 11692–11711, doi:10.1002/2015JD024637, 2016.

Tulet, P., Di Muro, A., Colomb, A., Denjean, C., Duflot, V., Arellano, S., Foucart, B., Brioude, J., Sellegri, K., Peltier, A., Aiuppa, A., Barthe, C., Bhugwant, C., Bielli, S., Boissier, P., Boudoire, G., Bourrianne, T., Brunet, C., Burnet, F., Cammas, J.-P., Gabarrot, F., Galle, B., Giudice, G., Guadagno, C., Jeamblu, F., Kowalski, P., Leclair de Bellevue, J., Marquestaut, N., Mékies, D., Metzger, J.-M., Pianezze, J., Portafaix, T., Sciare, J., Tournigand, A., and Villeneuve, N.: First results of the Piton de la Fournaise STRAP 2015 experiment: multidisciplinary tracking of a volcanic gas and aerosol plume, Atmos. Chem. Phys., 17, 5355-5378, https://doi.org/10.5194/acp-17-5355-2017, 2017.

Vakkari, V., Laakso, H., Kulmala, M., Laaksonen, A., Mabaso, D., Molefe, M., Kgabi, N., and Laakso, L.: New particle formation events in semi-clean South African savannah, Atmos. Chem. Phys., 11, 3333-3346, https://doi.org/10.5194/acp-11-3333-2011, 2011.

Vanhanen, J., Mikkilä, J., Lehtipalo, K., Sipilä, M., Manninen, H. E., Siivola, E., Petäjä, T. and Kulmala, M.: Particle Size Magnifier for Nano-CN Detection, Aerosol Sci. Technol., 45(4), 533–542, doi:10.1080/02786826.2010.547889, 2011.

Venzac, H., Sellegri, K., Laj, P., Villani, P., Bonasoni, P., Marinoni, A., Cristofanelli, P., Calzolari, F., Fuzzi, S. and Decesari, S.: High frequency new particle formation in the Himalayas, Proc. Natl. Acad. Sci., 105(41), 15666–15671, 2008.

Vigouroux, C., Stavrakou, T., Whaley, C., Dils, B., Duflot, V., Hermans, C., Kumps, N., Metzger, J.-M., Scolas, F., Vanhaelewyn, G., Müller, J.-F., Jones, D. B. A., Li, Q., and De Mazière, M.: FTIR time-series of biomass burning products (HCN, C2H6, C2H2, CH3OH, and HCOOH) at Reunion Island (21° S, 55° E) and comparisons with model data, Atmos. Chem. Phys., 12, 10367-10385, https://doi.org/10.5194/acp-12-10367-2012, 2012.

Wiedensohler, A., Birmili, W., Nowak, A., Sonntag, A., Weinhold, K., Merkel, M., Wehner, B., Tuch, T., Pfeifer, S., Fiebig, M., Fjäraa, A. M., Asmi, E., Sellegri, K., Depuy, R., Venzac, H., Villani, P., Laj, P., Aalto, P., Ogren, J. A., Swietlicki, E.,

Williams, P., Roldin, P., Quincey, P., Hüglin, C., FierzSchmidhauser, R., Gysel, M., Weingartner, E., Riccobono, F., Santos, S., Grüning, C., Faloon, K., Beddows, D., Harrison, R., Monahan, C., Jennings, S. G., O'Dowd, C. D., Marinoni, A., Horn, H.-G., Keck, L., Jiang, J., Scheckman, J., Mcmurry, P. H., Deng, Z., Zhao, C. S., Moerman, M., Henzing, B., De Leeuw, G., Löschau, G. and Bastian, S.: Mobility particle size spectrometers: harmonization of technical standards and data structure to facilitate high quality long-term observations of atmospheric particle number size distributions, Atmospheric Meas. Tech., 5, 657–685, doi:10.5194/amt-5-657-2012, 2012.

Yan, C., Dada, L., Rose, C., Jokinen, T., Nie, W., Schobesberger, S., Junninen, H., Lehtipalo, K., Sarnela, N., Makkonen, U., Garmash, O., Wang, Y., Zha, Q., Paasonen, P., Bianchi, F., Sipilä, M., Ehn, M., Petäjä, T., Kerminen, V.-M., Worsnop, D. R., and Kulmala, M.: The role of H2SO4-NH3 anion clusters in ion-induced aerosol nucleation mechanisms in the boreal forest, Atmos. Chem. Phys., 18, 13231-13243, https://doi.org/10.5194/acp-18-13231-2018, 2018.

Yli-Juuti, T., Nieminen, T., Hirsikko, A., Aalto, P. P., Asmi, E., Hõrrak, U., Manninen, H. E., Patokoski, J., Dal Maso, M., Petäjä, T., Rinne, J., Kulmala, M., and Riipinen, I.: Growth rates of nucleation mode particles in Hyytiälä during 2003−2009: variation with particle size, season, data analysis method and ambient conditions, Atmos. Chem. Phys., 11, 12865-12886, https://doi.org/10.5194/acp-11-12865-2011, 2011.

Zelenski, M., Taran, Y., and Galle, B.: High emission rate of sulfuric acid from Bezymianny volcano, Kamchatka, Geophys. Res. Lett., 42, 7005–7013, doi:10.1002/2015GL065340, 2015.